Digital Troposcatter Transmission and Modulation Theory

By E. D. SUNDE

(Manuscript received May 20, 1963)

In tropospheric scatter transmission beyond the horizon, the amplitude, phase and frequency of a received sine wave exhibit random fluctuations owing to variable multipath transmission and noise. The probability of errors in digital transmission over such random multipath media has been dealt with in the literature on the premise of flat Rayleigh fading over the band occupied by the spectrum of transmitted pulses. This is a legitimate approximation at low transmission rates, such that the pulse spectrum is adequately narrow, but not at high digital transmission rates. The probability of errors is determined here also for high transmission rates, such that selective fading over the pulse spectrum band must be considered. Such selective fading gives rise to pulse distortion and resultant intersymbol interference that may cause errors even in the absence of noise.

Troposcatter transmission can be approximated by an idealized multipath model in which the amplitudes of signal wave components received over different paths vary at random and in which there is a linear variation in transmission delay with a maximum departure $\pm\Delta$ from the mean delay. Various statistical transmission parameters are determined on this premise, among them the probability distribution of amplitude and phase fluctuations and of derivatives thereof with respect to time and with respect to frequency. The probability of errors in the absence of noise owing to such fluctuations is determined together with the probability of errors owing to noise, for digital transmission by binary PM and FM. Charts are presented, from which can be determined the combined probability of errors from various sources, as related to the transmission rate and certain basic parameters of troposcatter links.

CONTENTS

Page

Introduction 145
I. Channel Transmission Characteristics 148
1.1 General

1.2 Tropospheric Scatter Waves
1.3 Troposcatter Transmittance
1.4 Transmission Loss Fluctuations
1.5 Time Autocorrelation Function of Transmittance
1.6 Observed Time Autocorrelation (Fading Bandwidth)
1.7 Frequency Correlation Function of Transmittance
1.8 Differential Transmission Delay
1.9 Observed Frequency Variation in Transmittance
II. Transmittance Variations with Time 160
2.1 General
2.2 Amplitude and Phase Distributions
2.3 Distribution of Envelope Slopes (r')
2.4 Distribution of Phase Derivative (φ')
2.5 Distribution of Frequency Derivative (φ'')
III. Transmittance Variations with Frequency 165
3.1 General
3.2 Amplitude and Phase Distributions
3.3 Slope in Amplitude Characteristic ($\dot{r}$)
3.4 Envelope Delay Distribution ($\dot{\varphi}$)
3.5 Distribution of Linear Delay Distortion ($\ddot{\varphi}$)
IV. Errors from Transmittance Variations with Frequency 169
4.1 General
4.2 Carrier Pulse Transmission Characteristic
4.3 Ideal Pulse Spectra and Pulse Shapes
4.4 Linear Variation in Amplitude Characteristic
4.5 Probability of Errors from Linear Amplitude Dispersion
4.6 Linear Variation in Envelope Delay
4.7 Maximum Tolerable Linear Delay Distortion
4.8 Probability of Errors from Linear Delay Distortion
V. Errors from Transmittance Variations with Time 181
5.1 General
5.2 Amplitude Variations
5.3 Carrier Frequency Variations
5.4 Frequency Variation over a Signal Interval
5.5 Error Probability in Binary FM
5.6 Phase Variations over a Signal Interval
5.7 Error Probabilities in PM
VI. Errors from Noise with Flat Rayleigh Fading 189
6.1 General
6.2 Signal-to-Noise Ratios
6.3 Error Probability with Flat Rayleigh Fading
6.4 Binary PM with Synchronous Detection
6.5 Binary PM with Differential Phase Detection
6.6 Binary FM with Dual Filter Detection
6.7 Binary FM with Frequency Discriminator Detection
6.8 Binary AM with Ideal Gain Control
6.9 Binary AM with Optimum Fixed Threshold Detection
6.10 Combined Rayleigh and Slow Log-Normal Fading
VII. Combined Error Probability 196
7.1 General
7.2 Combined Error Probability
7.3 Binary PM with Differential Phase Detection
7.4 Error Probability Chart for Binary PM
7.5 Binary FM with Frequency Discriminator Detection
7.6 Error Probability Chart for Binary FM
7.7 Diversity Transmission Methods
7.8 Error Probabilities with Equal Gain Diversity
7.9 Error Probabilities with Selection Diversity
7.10 Multiband Digital Transmission
VIII. Summary 205
8.1 Troposcatter Transmittance
8.2 Variations in Transmittance with Time

8.3 Variations in Transmittance with Frequency
8.4 Errors from Selective Fading
8.5 Errors from Nonselective Rayleigh Fading
8.6 Errors from Random Noise
8.7 Combined Error Probability
8.8 Basic Approximations
8.9 Comparison with Recent Related Publications
IX. Acknowledgments 209
Appendix: Transmittance of Troposcatter Channels 210
References 214

INTRODUCTION

In tropospheric transmission beyond the horizon, narrow-beam transmitting and receiving antennas are used in a frequency range from about 400 to 10,000 megacycles. The received wave can be considered the sum of a large number of components of varying amplitudes, resulting from a multiplicity of reflections within the common volume at the intersection of the antenna beams. These various components arrive with different transmission delays owing to path-length differences, and each will exhibit a variation in amplitude owing to structural changes within the common volume, caused largely by winds. When a steady-state sine wave is transmitted, the received wave will consequently exhibit variations in its envelope and phase, commonly referred to as fading. When a signal wave is transmitted, its various frequency components will suffer unwanted amplitude and phase variations with resultant transmission impairments that depend on the particular carrier modulation method. These impairments are discussed herein for digital transmission by carrier phase and frequency modulation.

Various properties of the transmittance of troposcatter channels have been dealt with in several publications.[1,2,3,4] These properties include the expected average path loss and systematic seasonal variations from the average, together with the probability distributions of slow and rapid fading or fluctuations from the mean. Other important properties from the standpoint of systems design and performance are the distribution of duration of fades and the fading rapidity or rate.

The above various properties relate to transmittance variations with time at a particular frequency. Of basic importance is also the variation in transmittance with frequency at any instant, i.e., the amplitude and phase characteristics of trophospheric channels. These will be highly variable quantities, as illustrated in Fig. 1. At a fixed instant the characteristics may be as indicated in Fig. 1(a) and at a later instant as in Fig. 1(b). Such fluctuations will give rise to a distortion of the spectrum of received signals, with resultant transmission impairments of various kinds, depending on the modulation method. In addition,

random noise at the receiver input must be considered as in conventional stable channels. Owing to the above random fluctuations, diversity transmission is ordinarily required to insure adequate performance.

At present, frequency modulation is used for transmission of multiplexed voice channels over troposcatter links. With this method, pronounced intermodulation noise is encountered[5,6] owing to the types of transmittance variations with frequency indicated in Fig. 1. With digital transmission, these variations will give rise to pulse distortion and resultant intersymbol interference that may severely limit the transmission rate.

In evaluation of error probabilities in digital transmission, it is necessary to consider variations in the average path loss over a convenient period, such as an hour, relative to the average over a much longer period, say a month. These slow fluctuations in loss are closely approximated by the log-normal law; i.e., the loss in db follows the normal law.[1] In addition, consideration must be given to rapid fluctuations in loss relative to the above hourly averages. These are closely approximated by the Rayleigh law, which also applies for the envelope of narrow-band random noise. They are ordinarily more important than slow fluctuations, particularly in digital transmission, in that they cannot be fully compensated for by automatic gain control. Nearly all theoretical analyses of error probabilities in digital transmission over fading channels are based on a Rayleigh distribution together with various other simplifying assumptions, as outlined below.

The simplest assumption is flat or nonselective Rayleigh fading over the channel band, in conjunction with a sufficiently slow fading rate such that changes over a few pulse intervals can be disregarded. These

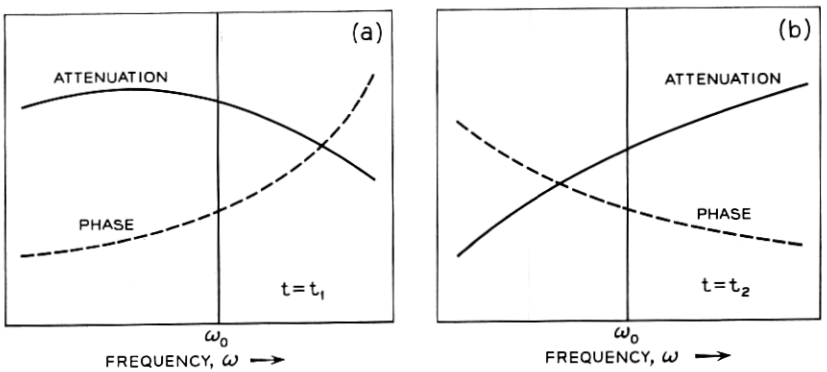

Fig. 1 — Illustrative variations in attenuation and phase characteristics with frequency at two instants t_1 and t_2.

are legitimate premises in transmission over line-of-sight radio links, where fading is much slower than on tropospheric links and is virtually nonselective over rather wide bands. With these simplifying assumptions Turin[7] has determined error probabilities in binary transmission over noisy channels with ideal synchronous (coherent) detection and envelope (noncoherent) detection. His analysis includes the effect of correlation between successive pulses and also postulates a nonfading signal component, such that the results in one limit also apply for nonfading channels.

On the same premise of slow, flat Rayleigh fading, Pierce[8] has determined the optimum theoretical diversity improvement for frequency shift keying with dual filter reception employing coherent and noncoherent detection of the filter outputs. Dual filter detection is ordinarily assumed in place of the usual method of frequency discriminator detection that does not lend itself as readily to theoretical analysis.

The error probability with two-phase and four-phase modulation with differential phase detection has been determined by Voelcker[9] on the premise of flat Rayleigh fading at such a rate that the change in phase over a pulse interval must be considered. Moreover, he considers the probability of both single and double digital errors, with both single and dual diversity transmission.

Voelcker's analysis is applicable to transmission at a sufficiently slow rate such that amplitude and phase distortion can be ignored over the relatively narrow band of the pulse spectra. However, it does not apply to high-speed digital transmission that requires sufficiently wide pulse spectra such that the amplitude and phase distortion indicated in Fig. 1 must be considered. For this case the duration of pulses will be so short that the phase changes considered by Voelcker can be disregarded. Instead, it now becomes necessary to take into account pulse distortion and resultant intersymbol interference caused by the erratic variations with frequency in the amplitude and phase characteristics illustrated in Fig. 1. An evaluation is made herein of error probabilities on the latter account, which has not been considered in previous publications.*

From the solutions for the above two limiting cases of low and high transmission rates, it is possible by simple graphical methods to estimate the error probability for the general case in which both time and frequency variations in the amplitude and phase characteristics must be considered. Charts are presented of error probabilities in digital transmission by binary PM and FM as related to various basic parameters of tropospheric scatter links and of the signals. Among these

* For reference to a recent related paper, see Section 8.9.

parameters are the average signal-to-noise ratio, the bandwidth of the pulse spectrum, the fading bandwidth of the troposcatter link, and the maximum departure from the mean transmission delay, which is related to the length of the link and the antenna beam angles.

The analysis shows that a principal source of pulse distortion and resultant transmission impairments is a component of quadratic phase distortion. On this premise, an evaluation has been made in a companion paper* of intermodulation distortion in analog transmission by FM and PM, that conforms well with the results of measurements.[5,6]

I. CHANNEL TRANSMISSION CHARACTERISTICS

1.1 *General*

Transmission performance with any modulation method depends on the statistical properties of the signals and of channel noise, together with various properties of the channel transmittance or transmission-frequency characteristic. When the latter varies with time, the usual methods of determining network response to specified input waves must be modified in various respects, that result in appreciable complications in the analytical methods[10] and in certain conceptual difficulties. However, when the time variations in transmittance are slow in relation to those in the input waves, it is legitimate to assume that the transmittances are constant over an appreciable number of pulse intervals. With relatively slow random fluctuations as encountered in troposcatter systems at representative transmission rates, it is thus permissible to determine the responses for various essentially time invariant transmittances that can be encountered. In evaluating transmission performance, the various transmittances that can be encountered must be weighted or averaged statistically in a manner that depends on the signal properties and the modulation method.

Among the statistical properties of troposcatter transmittances are the probability distribution of the envelope of received carrier waves together with the autocorrelation function of the envelope with respect to time and with respect to frequency. These are discussed here, while other statistical properties will be considered in later sections.

1.2 *Tropospheric Scatter Waves*

To determine an appropriate model for the random process in tropospheric scatter transmission, it is necessary to consider the physics

* See part 2 of this issue of the B.S.T.J., to appear.

of this phenomenon, as dealt with in various publications. Though these may differ in their assumptions regarding the exact mechanism of the reflections, they appear to agree that they occur as a result of heterogeneities within the common antenna volume indicated in Fig. 2. If the transmission medium were uniform, no reception would be possible. Owing to the numerous heterogeneities in the common volume, a very large number of reflections will occur, and the received wave can be considered the sum of a large number of components of different amplitudes and different transmission delays. Over any short interval, the envelope of a received sine wave will depend on the frequency, as will the phase. Because of variations in the heterogeneities caused largely by winds, the envelope and phase of a received carrier will vary with time.

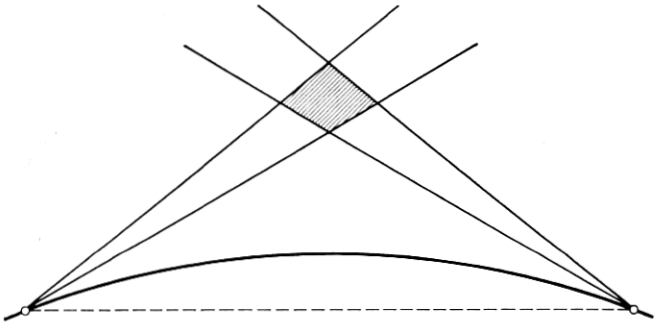

Fig. 2 — Illustrative antenna beams and common antenna volume.

The transmittance of troposcatter channels is dealt with here, based on an idealized model discussed further in the Appendix, and certain statistical parameters obtained from experimental data are discussed. Two limiting cases that permit simplified analysis are considered. In one case the transmission band is assumed sufficiently narrow, such that the attenuation characteristic can be considered constant and the phase characteristic linear over the narrow band. There will then be fluctuations with time in the attenuation accompanied by independent variations in the slope of the phase characteristic, a condition referred to as nonselective flat fading and ordinarily assumed in random multipath digital transmission theory. The other limiting case is that of digital transmission at a sufficiently high rate so that time variations in the transmittance can be disregarded over an appreciable number of pulse intervals. In this case it is necessary to consider erratic variations with frequency in both the attenuation and phase characteristics.

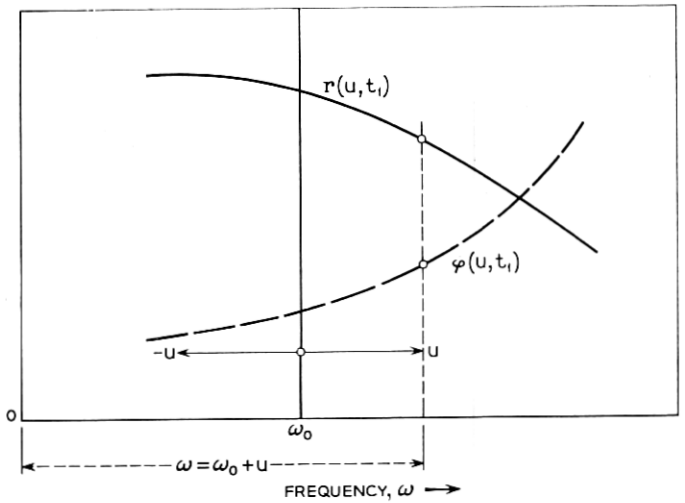

Fig. 3 — Illustrative dependence of envelope and phase of transmittance with frequency u from a reference frequency ω_0 at a specified time t_1 .

1.3 *Troposcatter Transmittance*

Let a sine wave of frequency ω be transmitted, and let $\omega = \omega_0 + u$, as indicated in Fig. 3, where ω_0 is a conveniently chosen reference frequency. In complex notation the received wave is then of the general form

$$e(u,t) = r(u,t) \exp[-i\varphi(u,t)] \exp(i\omega t) \tag{1}$$

where $r(u,t)$ and $\varphi(u,t)$ are random variables of the time t for a fixed ω or u, and of u for a fixed time t. The channel transmittance is then

$$T(u,t) = r(u,t) \exp[-i\varphi(u,t)]. \tag{2}$$

The following general relations apply

$$r(u,t) = [U^2(u,t) + V^2(u,t)]^{\frac{1}{2}} \tag{3}$$

$$\varphi(u,t) = \tan^{-1} [V(u,t)/U(u,t)]. \tag{4}$$

As shown in the Appendix, in the case of idealized tropospheric channels the functions U and V can be represented in the following form

$$U(u,t) = \sum_{j=-\infty}^{\infty} a_j(t) \frac{\sin (j\pi - u\Delta)}{j\pi - u\Delta} \tag{5}$$

$$V(u,t) = \sum_{j=-\infty}^{\infty} b_j(t) \frac{\sin(j\pi - u\Delta)}{j\pi - u\Delta} \tag{6}$$

where

Δ = maximum departure from mean transmission delay owing to path length differences.

In (5) and (6) the coefficients $a_j(t)$ and $b_j(t)$ vary at random with time t and for a given t vary at random with j. Owing to the latter variation with j, there will be a random variation in U and V with the frequency u taken in relation to the reference frequency ω_0.

Equations for an idealized troposcatter channel, as given in the Appendix, show that $a_j(t)$ is related to the sum $A(x,t) + A(-x,t)$ of two random processes and $b_j(t)$ to the difference $A(x,t) - A(-x,t)$. The two random processes $A(x,t)$ and $A(-x,t)$ will have equal rms amplitudes, in which case $a_j(t)$ and $b_j(t)$ will have zero correlation coefficient. They will then also be independent random variables, provided $A(x,t)$ and $A(-x,t)$ have a Gaussian probability distribution, which appears to be a legitimate approximation since each will be the sum of waves from a large number of reflections.

A further assumption underlying (5) and (6) is that there is an infinite number of transmission paths. An additional approximation that will be made in the following analysis is that there will be independent random fluctuations in the signal components received over the various paths. Actually there will be some correlation between the fluctuations, particularly for paths with small separation. In effect, there will be a limited number of essentially independently fading paths.

The above assumptions entail certain statistical properties of troposcatter channels, as outlined below for time and frequency variations.

1.4 *Transmission Loss Fluctuations*

On troposcatter links there is a certain average transmission loss over a year, which depends on the length of the link, on the properties of the terrain and on climatic conditions. Experimental data indicate that there will be systematic monthly and seasonal departures from this yearly average, owing principally to slow temperature changes. The average loss during a winter month may thus be up to 20 db greater than the average during a summer month. That is, the departure in transmission loss from the yearly mean may be ± 10 db.

During each month there will be a more or less random fluctuation

in the hourly average loss from the mean of the month. This fluctuation has been found to be almost independent of frequency and seems to be associated with the variations in average refraction of the atmosphere and resultant variation in the bending of beams. This fluctuation in the hourly average loss relative to the monthly average has been found to follow closely the log-normal law. That is to say, let the monthly median loss be

$$\alpha_m = -\ln \bar{r}_m^2 \tag{7}$$

and the hourly average loss be

$$\alpha = -\ln \bar{r}^2 \tag{8}$$

where $\ln = \log_\epsilon$, $\bar{r}_m$ is the monthly rms amplitude of the envelope $r(u,t)$, and $\bar{r}$ the rms amplitude over an hour. (Other reference times could have been chosen, as will appear below.)

The probability that the average hourly loss exceeds a specified value $\alpha_1 = \ln \bar{r}_1^2$ is then given by

$$P(\alpha \geqq \alpha_1) = \frac{1}{2}\left[1 - \operatorname{erf} \frac{\alpha_1 - \alpha_m}{\sqrt{2}\sigma_\alpha}\right] \tag{9}$$

where erf is the error function and σ_α the standard deviation in transmission loss expressed in nepers, when α and α_m are expressed in nepers as above. For links 100 to 200 miles in length, a representative value of σ_α appears to be about 0.9 neper (8 db).

In addition to the above slow variations in the average hourly loss, there will be more rapid fluctuations in the envelope $r(u,t)$, owing to changes in the multipath transmission structure caused principally by winds. This type of fluctuation follows a Rayleigh distribution law. According to this law the probability that the instantaneous value r of the envelope exceeds a specified value r_1 is

$$P(r > r_1) = \exp(-r_1^2/\bar{r}^2) \tag{10}$$

where $\bar{r}$ is the hourly rms value referred to above.

It may be noted that while the log-normal law for slow variation has been determined solely by measurements, the Rayleigh law for rapid fluctuations follows by theory when the received wave is the sum of a large number of variable components.

The probability distribution (10) can be related to the monthly rms value of $r(u,t)$ with the aid of (9) by

$$P(r > r_1) = \int_0^\infty p(\bar{r}) \exp(-r_1^2/\bar{r}^2)\, d\bar{r} \tag{11}$$

where $p(\bar{r})$ is the probability density function corresponding to (9), which is

$$p(\bar{r}) = \frac{1}{\sqrt{2\pi}\sigma_\alpha \bar{r}} \exp\{-[\ln \bar{r}^2/r_m{}^2]^2/2\sigma_\alpha{}^2\}. \tag{12}$$

It will be recognized that (11) will yield the same result regardless of the period over which the rms value $\bar{r}$ is taken, since $\bar{r}$ simply plays the role of an intermediate parameter that disappears after integration.

The above probability functions relating to average loss or the distribution of the instantaneous values of $r(u,t)$, are independent of the frequency. In addition to the above distribution there are others which are important from the standpoint of transmission systems design and performance, as discussed in the following section.

1.5 *Time Autocorrelation Functions of Transmittance*

Expressions for the probabilities of rapid changes in the amplitude and phase of the transmittance with time will be considered in Section II. These involve the autocorrelation functions of the components U and V defined by (5) and (6), or the corresponding power spectra. Both have the same autocorrelation function and power spectrum, so that only $U(u,t)$ needs to be considered.

The time autocorrelation function of $U(u,t)$ depends on the variation in $a_j(t)$ with time. These are related to changes in the physical structure of the common volume and to resultant variations in the heterogeneities that are responsible for tropospheric transmission. The rate at which these occur depends on the velocity and directions of winds and on temperature changes. Under these conditions the autocorrelation function will vary with time, and it becomes necessary to consider a certain median autocorrelation function and corresponding power spectrum, as discussed in Section 1.6.

Let $\Psi(\tau)$ be the autocorrelation function of variations in $U(u,t)$ with t. The corresponding one-sided power spectrum is then

$$W(\gamma) = \frac{2}{\pi} \int_0^\infty \Psi(\tau) \cos \gamma\tau \, d\tau \tag{13}$$

where γ is used to designate the radian frequency of spectral components to avoid confusion with the frequency ω of the transmitted wave.

The autocorrelation function $\Psi(\tau)$ or the corresponding power spectrum $W(\gamma)$ of the components U and V cannot be determined as readily by measurements as the autocorrelation function $\Psi_r(\tau)$ of the envelope. The latter is related to $\Psi(\tau)$ by[11]

$$\Psi_r(\tau) = \Psi(0)\{2E[\kappa(\tau)] - [1 - \kappa^2(\tau)]K[\kappa(\tau)]\} \tag{14}$$

where

$$\kappa(\tau) = \Psi(\tau)/\Psi(0) \tag{15}$$

E = complete elliptic integral of second kind

K = complete elliptic integral of first kind.

For $\tau = 0$, $\Psi_r(0) = 2\Psi(0)$. Hence the autocorrelation coefficient of the envelope can be written

$$\kappa_r(\tau) = E[\kappa(\tau)] - \tfrac{1}{2}[1 - \kappa^2(\tau)]K[\kappa(\tau)]. \tag{16}$$

With the aid of (16), the autocorrelation coefficient $\kappa(\tau)$ of each quadrature component can be determined from measurements of $\kappa_r(\tau)$.

1.6 *Observed Time Autocorrelation*

Observations of the autocorrelation function of rapid fluctuations indicate that the autocorrelation function $\Psi(\tau)$ of the components U and V is nearly Gaussian and is given by

$$\Psi(\tau) = \Psi(0) \exp(-\sigma^2\tau^2/2). \tag{17}$$

The corresponding power spectrum obtained from (13) is

$$W(\gamma) = \Psi(0)(2/\pi\sigma^2)^{\frac{1}{2}} \exp(-\gamma^2/2\sigma^2) \tag{18}$$

where $\Psi(0)$ is the average power in each component as obtained with $\tau = 0$ in (17) .

The equivalent bandwidth of a flat power spectrum $W(\gamma) = W(0)$ is given by

$$\bar{\gamma} = \sqrt{(\pi/2)}\,\sigma \approx 1.25\sigma. \tag{19}$$

As noted in Section 1.5, there will be a certain median autocorrelation function and corresponding median values of the power spectrum, of σ and of γ. Measurements[2] indicate that these median values depend on the antenna beamwidths and that the fading rate is not quite proportional to frequency. Furthermore, there can be appreciable departure from the median values. From measurements of the median number of fades per minute, the median value of σ can be determined, with the aid of equation (26) in Ref. 2. These measurements indicate that for a particular antenna arrangement $\sigma \approx 0.1$ cps at 460 mc and about 1.3 cps at 4110 mc. The corresponding equivalent bandwidths of a flat power spectrum are thus $\bar{\gamma} \approx 0.125$ cps, or 0.8 radian/sec. at 460 mc, and $\bar{\sigma} \approx 1.6$ cps, or about 10 radians/sec. at 4110 mc. The measurements

further indicate that there is a probability of about 0.01 that the fading rate exceeds the median value by a factor of about 7 at 460 mc and a factor of about 3.5 at 4110 mc.

1.7 *Frequency Correlation Function of Transmittance*

Returning to (5) and (6), let the time t be fixed, and consider variations in U and V with u. The coefficients a_j and b_j will then have certain values that vary with j, and there will be a certain variation in U and V with u. At a different time there will be another set of coefficients and a different variation with u. The form of (5) and (6) indicates that if u is regarded as a time variable and Δ as a frequency, $U(u)$ would be the variation in time owing to impulses of amplitudes a_j and b_j impinging at time intervals π on a flat low-pass filter of bandwidth Δ. That is to say, the autocorrelation function of components U and V for a difference $\nu = \omega_2 - \omega_1$ in frequency is

$$\Psi(\nu) = \Psi(0)(\sin \nu\Delta/\nu\Delta). \tag{20}$$

The corresponding power spectrum of the variation in U and V with frequency δ is

$$W(\delta) = \frac{2}{\pi}\int_0^\infty \Psi(\nu) \cos \nu\delta \, d\nu \tag{21}$$

$$\begin{aligned} &= \Psi(0) \qquad \text{for} \qquad 0 < \delta < \Delta \\ &= 0 \qquad\quad \text{for} \qquad \Delta < \delta. \end{aligned} \tag{22}$$

When $\Psi(\nu)$ is given, it is possible to determine the autocorrelation function $\Psi_r(\nu)$ for variations in $r(u,t)$ with u. Expression (14) applies with ν in place of τ, for the autocorrelation function of time variation with frequency.

For an autocorrelation function (20), the corresponding correlation coefficient is

$$\kappa(\nu) = (\sin \nu\Delta/\nu\Delta). \tag{23}$$

The corresponding autocorrelation coefficient of the envelope, as obtained from (16), is

$$\kappa_r(\nu) = E\left(\frac{\sin \nu\Delta}{\nu\Delta}\right) - \frac{1}{2}\left[1 - \frac{\sin^2 \nu\Delta}{(\nu\Delta)^2}\right] K\left(\frac{\sin \nu\Delta}{\nu\Delta}\right). \tag{24}$$

For various values of $\nu\Delta$ the correlation function of the envelope is given in Table I and is shown in Fig. 4.

TABLE I — AUTOCORRELATION FUNCTION OF ENVELOPE

$\nu\Delta = 0$	$\pi/2$	π	$3\pi/2$	∞
$\kappa_r(\nu) = 1$	0.9	$\pi/4$	0.78	$\pi/4$

The autocorrelation functions (23) and (24) apply for certain idealized conditions outlined in the Appendix and in Section 1.3. For one thing, the average power received over each elementary path is assumed the same. For another, a linear variation in the transmission delay with angular deviation from the mean paths is assumed, with maximum departures $\pm\Delta$ from the mean delay. Furthermore, an infinity of transmission paths is assumed, with independent random fluctuations in the

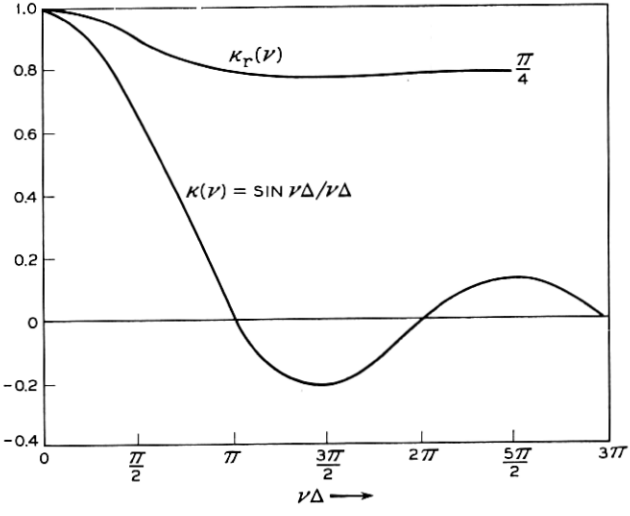

Fig. 4 — Frequency autocorrelation coefficient $\kappa_r(\nu)$ of envelope for autocorrelation coefficient $\kappa(\nu)$ of components U and V.

signal components received over the various paths, though there will be some correlation between the fluctuations in the signal components received over various paths.

In spite of the various approximations, it appears possible to obtain a reasonably satisfactory conformance with the results of measurements of the autocorrelation functions of the envelope, as shown in Section 1.9.

1.8 *Differential Transmission Delay* Δ

Exact determination of the equivalent maximum departure from the mean transmission delay requires consideration of the beam patterns as affected by scattering. On the approximate basis of equivalent beam angles α, the following relation applies, with notation as indicated in Fig. 5

$$\Delta \approx \frac{L}{v} \frac{\alpha + \beta}{2} \left(\theta + \frac{\alpha + \beta}{2} \right) \tag{25}$$

where $\beta \leqq \alpha$, v is the velocity of propagation in free space, L is the length of the link, and

$$\theta = \frac{L}{2R} = \frac{L}{2R_0K} \tag{26}$$

where R_0 is the radius of the earth and the factor K is ordinarily taken as 4/3.

The equivalent beam angle α from midbeam to the 3-db loss point depends on the free-space antenna beam angle α_0 and on the effect of scatter, which is related in a complex manner to α_0 and the length L, or alternately θ. Narrow-beam antennas as now used in actual systems are loosely defined by $\alpha_0 \leqq 2\theta/3$. For these $\alpha \approx \alpha_0$ on shorter links, while on longer links $\alpha > \alpha_0$ owing to beam-broadening by scatter. Analytical determination of α for longer links appears difficult, and only

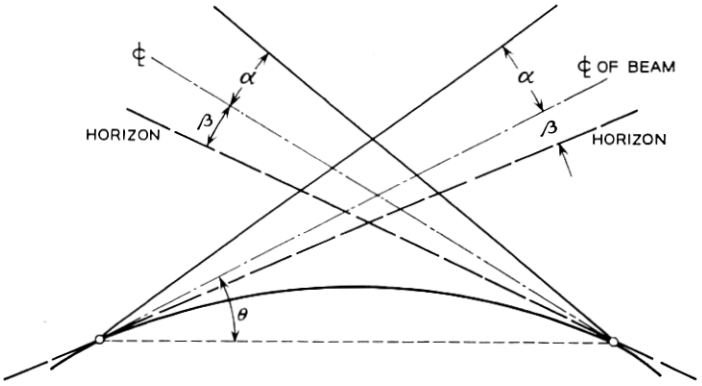

Fig. 5 — Definition of antenna beam angles α, take-off angle β and chord angle θ to midbeam. With different angles at the two ends, the mean angles are used in expressions for Δ. In applications to actual beams, α would be the angle to the 3-db loss point.

limited experimental data are available at present. For broad-beam antennas, $\alpha_0 > 2\theta/3$ and beam-broadening by scatter is in theory inappreciable.

By way of numerical example, let $L = 170$ miles and $K = 4/3$, in which case $\theta = 0.016$ radian. Since $\alpha_0 = 0.004$ radian $\ll 2\theta/3$, it is permissible to take $\alpha = \alpha_0$. With $\beta \approx \alpha_0$, (25) gives $\Delta = 0.08 \times 10^{-6}$ second.

1.9 *Observed Frequency Variations in Transmittance*

In Fig. 6 is indicated the shapes of the envelope vs frequency variations that can be obtained from (3) when the components U and V are given by (5) and (6). These fluctuations will vary with time but will have the characteristic shapes indicated in Fig. 6, which resemble shapes obtained in sweep-frequency measurements on a link of the length for which the above value of Δ applies.[2]

A better indication of the adequacy of the present idealized troposcatter model is obtained by comparing the autocorrelation coefficient of the envelope as given by (24) with the correlation coefficient derived from observations. In Fig. 7 is shown the theoretical coefficient for $\Delta = 0.08 \times 10^{-6}$ second together with coefficients obtained from three experimental runs considered representative.[2]

The bandwidth capability can be defined as the maximum baseband signal spectrum that can be received with some coherence between spectral components at the maximum and minimum frequencies. This

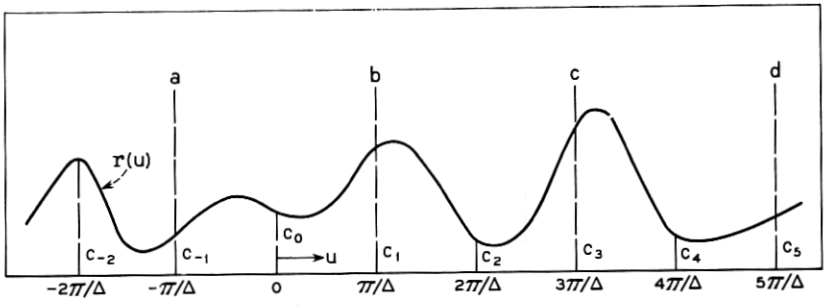

Fig. 6 — Illustrative rectified envelope vs frequency characteristic $r(u)$ obtained with expressions (5) and (6) in (3). The amplitudes c_j at the radian frequencies $u_j = j\pi/\Delta$ from the carrier are $c_j = (a_j^2 + b_j^2)^{\frac{1}{2}}$. The amplitude of the envelope at any intermediate frequency u depends on the amplitudes and phases of all c_j between $j = -\infty$ and $j = \infty$. In sweep-frequency measurements with a radian frequency sweep from $-\pi/\Delta$ to π/Δ from the carrier, the envelope variations might be like that in any of the intervals a-b, b-c, c-d, etc.

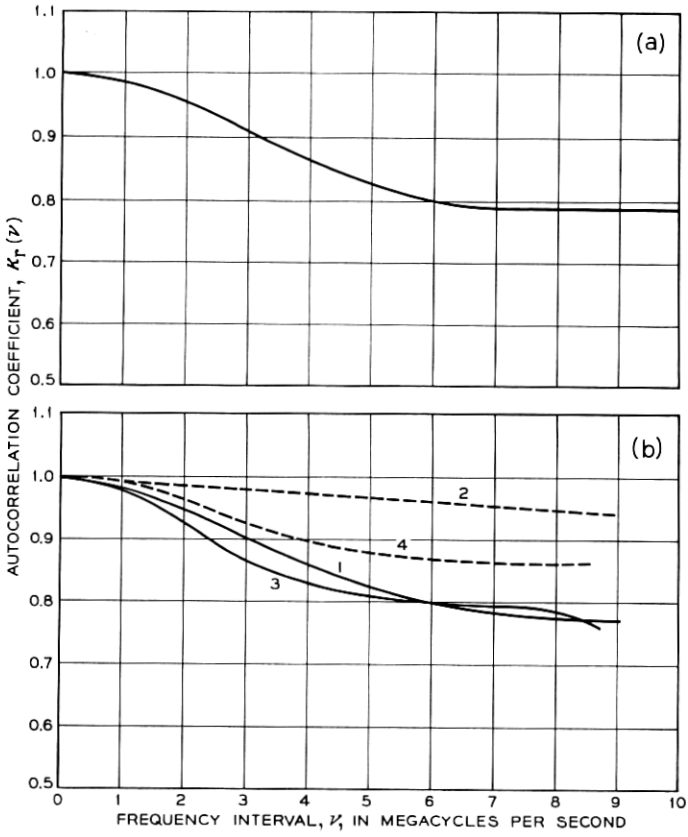

Fig. 7 — Theoretical vs observed envelope autocorrelation functions. Above: autocorrelation coefficient obtained from (24) with $\Delta = 0.08 \times 10^{-6}$ second. Below: autocorrelation coefficients given in Fig. 70 of Ref. 2 and derived from measurements of envelope variations with narrow-beam antennas on four days: 1. Sept. 13, 1957; 2. Sept. 30, 1957 (considered very unusual); 3. Oct. 15, 1957, and 4. Nov 8, 1957. The value of Δ derived from (25) for the experimental link is $\Delta = 0.08 \times 10^{-6}$ second.

bandwidth is equal to the separation between c_j and c_{j+1} in Fig. 6, which corresponds to the separation between null points in (23), for which $\kappa(\nu) = 0$ and $\kappa_r(\nu) = \pi/4$. It is given by $1/2\Delta$ cps and for $\Delta = 0.08 \times 10^{-6}$ second is 6.3 mc/second.

With a smaller spectral bandwidth, distortion will be reduced and transmission performance improved. A more realistic appraisal might be half the above maximum bandwidth, or 3.15 mc/second, for which $\kappa_r(\nu) = 0.9$. In Ref. 2 the criterion $k^2(\nu) = 0.6$ corresponding to $\kappa_r(\nu) =$

0.904 has been selected, and twice this spectrum bandwidth as required in double sideband transmission is quoted in Table VII of the reference.

The mathematical model represented by (3) to (6) is based on certain idealizations outlined in Section 1.7 and in the Appendix. It appears from the above that certain theoretical transmittance variations based on this model conform sufficiently well with observed variations for the model to be acceptable.* In order to determine expected performance with digital transmission, it is necessary to consider certain other statistical properties of tropospheric channels based on the above model, as discussed in sections that follow.

II. TRANSMITTANCE VARIATIONS WITH TIME

2.1 *General*

As discussed in Section 1.2, the transmission vs frequency characteristic of a tropospheric scatter channel is a highly variable quantity, as indicated in Fig. 1. One way of avoiding transmission impairments owing to variations in transmittance with frequency is to transmit by narrow-band modulation of a number of different carriers. The amplitude vs frequency characteristic can then be regarded as virtually constant over each narrow band, and the phase characteristic as linear, as indicated in Fig. 1. With this method, it is permissible to assume flat fading within each narrow band, but the various narrow channels will not fade independently. In addition to such flat fading there will be variations in the phase and frequency of each received carrier with time. Owing to the narrow bandwidth of each channel, the duration T of a signal or sampling interval may be relatively long, and it becomes necessary to consider the above amplitude, phase and frequency variations over this interval T. The probability distribution of these variations are basic to later considerations of various digital transmission methods and are discussed here. They can be obtained from expressions given by Rice for narrow-band random noise.[12]

2.2 *Amplitude and Phase Distributions*

Let the frequency ω and thus $u = \omega - \omega_0$ be fixed, and consider only time variations in r and φ. The probability density of φ is simply $p(\varphi) = 1/2\pi$, since each phase is equally probable. Since the components U and V are the sum of a very large number of independent random variables, in accordance with (5) and (6), each component U and V will have a

* This conclusion appears to be supported by the results of recent measurements of $\kappa(\nu)$ for a 100-mile path.[24]

normal law or Gaussian probability density. The probability density of the envelope in this case follows the Rayleigh law, and the probability that the envelope r exceeds a specified value r_1 is given by

$$P(r \geqq r_1) = \exp(-r_1^2/\bar{r}^2) \tag{27}$$

where $\bar{r}$ is the rms amplitude of the envelope or the transmittance taken over an appropriately long time.

The average received envelope power is in this case $\bar{r}^2 = \bar{S} = 2S$, where S is the average carrier power, i.e., the average power within the envelope. The probability that the received envelope power at any instant exceeds a specified value $\bar{S}_1 = 2S_1$ is

$$P(S > S_1) = \exp(-\bar{S}_1/\bar{S}) = \exp(-S_1/S). \tag{28}$$

The median value S_m of S is obtained from $P(S \geqq S_m) = \frac{1}{2}$, which gives $S_m = \bar{S} \ln 2$. Hence, in terms of the median value

$$P(S \geqq S_1) = \exp[-(S_1/S_m) \ln 2]. \tag{29}$$

The distribution represented by (28) or (29) is shown in Fig. 8.

The above distribution of rapid fades is to be distinguished from the distribution of slow variations in the envelope, or in attenuation, discussed in Section 1.4.

2.3 *Distribution of Envelope Slopes* (r')

One measure of the rapidity of the above amplitude variations is the fading bandwidth discussed in Section 1.6. From this fading bandwidth can be derived the probability distribution of the slope $r' = dr(t)/dt$ in the envelope.

The rapidity of changes in the envelope and phase depends on the time rate of change in the heterogeneities in the common volume — that is to say, the variations with respect to time of the coefficients $a_j(t)$ and $b_j(t)$ in (5) and (6). These changes are characterized by the autocorrelation function of $U(t)$ and $V(t)$, or by the corresponding power spectrum. When the power spectra of U and V are the same, and are specified, the probability distribution of $r' = dr(t)/dt$ and $\varphi' = d\varphi(t)/dt$ can be determined. These distributions are the same as for random noise of specified power spectrum. The probability that $|r'|$ exceeds a specified value $|r_1'|$ follows the normal law[12]

$$P(|r'| \geqq |r_1'|) = \operatorname{erfc}(k/2^{\frac{1}{2}}) \tag{30}$$

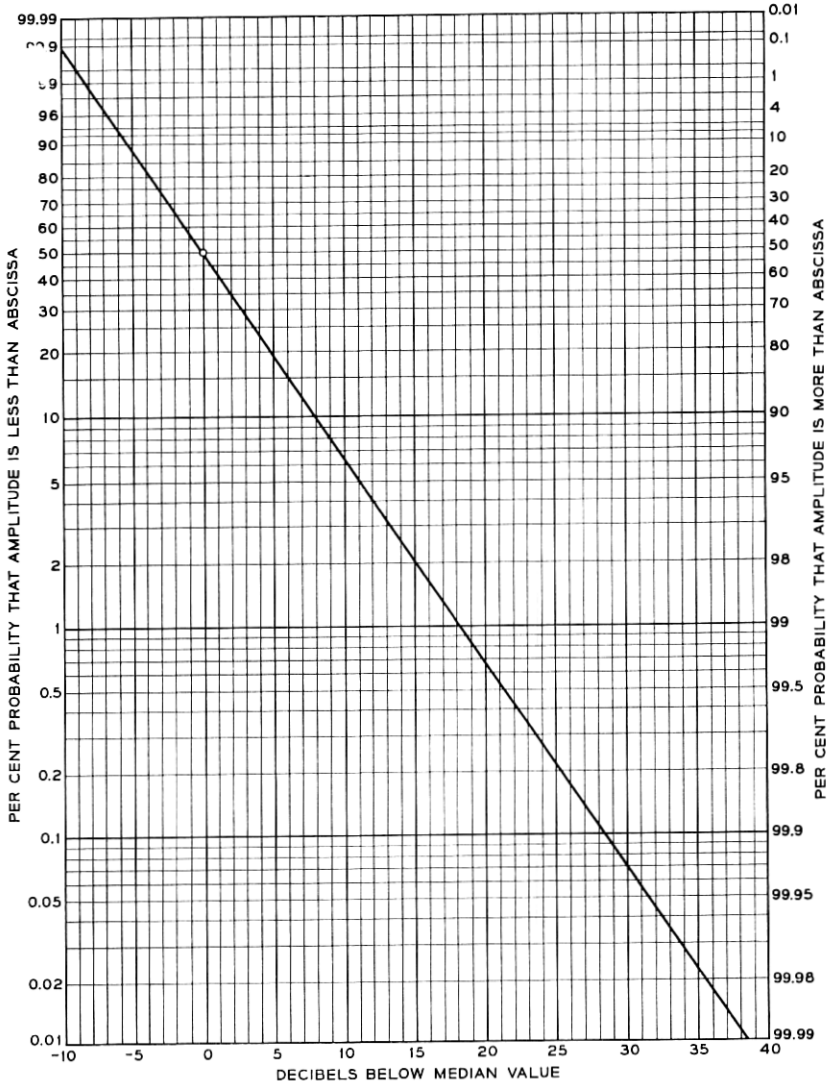

Fig. 8 — Rayleigh probability distribution of rapid fluctuations in envelope of a received carrier owing to multipath propagation.

in which

$$k = r_1'/\bar{r}'$$

$$\bar{r}' = \text{rms amplitude of } r'$$

$$= [\tfrac{1}{2}(b_2 - b_1^2/b_0)]^{\frac{1}{2}} \tag{31}$$

where

$$b_n = \int_0^\infty W(\gamma)\gamma^n \, d\gamma. \tag{32}$$

The above result (30) follows from equation (4.6) in Ref. 12 for $Q = 0$, by integration with respect to $R = r$ between 0 and ∞, and in turn with respect to $R' = r'$ between r_1' and ∞.

Expression (30) can alternatively be written

$$P[\,|\,r'\,|\,\geqq k\bar{r}'] = \text{erfc}\,(k/2^{\frac{1}{2}}). \tag{33}$$

In the particular case of flat power spectrum $W(\gamma) = W$ of bandwidth $\hat{\gamma}$, (32) gives

$$b_0 = W\hat{\gamma}; \qquad b_1 = W\hat{\gamma}^2/2; \qquad b_2 = W\hat{\gamma}^3/3$$

and (31) becomes

$$\bar{r}' = \bar{r}\hat{\gamma}/6^{\frac{1}{2}} \approx 0.405\bar{r}\hat{\gamma}. \tag{34}$$

The fading bandwidth in the above case is $\hat{\gamma}$ radians/second.

With a Gaussian spectrum (17) expression (32) gives

$$b_0 = \Psi(0); \qquad b_1 = \sigma(2/\pi)^{\frac{1}{2}}\Psi(0); \qquad b_2 = \sigma^2\Psi(0)$$

and (31) becomes

$$\bar{r}' = \bar{r}\sigma\left(\frac{1}{2} - \frac{1}{\pi}\right)^{\frac{1}{2}}$$

$$\approx 0.42\bar{r}\sigma \approx 0.34\bar{r}\bar{\gamma} \tag{35}$$

where $\bar{\gamma}$ is the equivalent bandwidth given by (19).

2.4 *Distribution of Phase Derivative* (φ')

In considering a small phase change $\Delta\varphi$, and over a small interval $\Delta\tau$, it is legitimate to use the probability distribution of the phase derivative $\varphi' = \Delta\varphi/\Delta\tau$, which is given by [Section 5 of Ref. 12]

$$P(|\,\varphi'\,| \geqq |\,\varphi_1'\,|) = 1 - \frac{k}{\sqrt{1 + k^2}} \tag{36}$$

in which

$$k = (b_0/b_2)^{\frac{1}{2}}\varphi_1' = (b_0/b_2)^{\frac{1}{2}}(\Delta\varphi_1/\Delta\tau) \tag{37}$$

where b_0 and b_2 are given by (32).

Expression (36) can alternatively be written

$$P(|\varphi'| \geqq k(b_2/b_0)^{\frac{1}{2}}) = 1 - \frac{k}{\sqrt{1+k^2}} \tag{38}$$

$$\approx \frac{1}{2k^2} \quad \text{for} \quad k \gg 1.$$

For a flat power spectrum $W(\gamma) = W$ of bandwidth $\hat{\gamma}$

$$(b_2/b_0)^{\frac{1}{2}} = \hat{\gamma}/3^{\frac{1}{2}} \approx 0.58\hat{\gamma}. \tag{39}$$

For a Gaussian spectrum (17)

$$(b_2/b_0)^{\frac{1}{2}} = \sigma \approx 0.8\bar{\gamma} \tag{40}$$

where $\bar{\gamma}$ is the equivalent bandwidth given by (19).

2.5 *Distribution of Frequency Derivative* (φ'')

The probability of exceeding a small variation $\Delta\omega$ in frequency over a brief interval $\Delta\tau$ can be determined from the probability distribution of $\varphi'' = \Delta\omega/\Delta\tau$.

The probability that φ'' exceeds a specified value φ_1'' is given by

$$\begin{aligned} P(|\varphi''| \geqq |\varphi_1''|) &= P(|\varphi''| \geqq kb_0/b_2) \\ &= 1 - \frac{2k}{\pi}\int_0^\infty \frac{dx}{[g(x)+k^2]g(x)} \\ &\quad - \frac{2}{\pi}\int_0^\infty \frac{\tan^{-1}(k/g^{\frac{1}{2}}(x))}{(1+x^2)^{\frac{3}{2}}}\,dx \end{aligned} \tag{41}$$

where

$$k = b_0\varphi_1''/b_2 \tag{42}$$

$$g(x) = (a - 1 + 4x^2)(1 + x^2) \tag{43}$$

$$a = b_0b_4/b_2^2. \tag{44}$$

Expression (41) is obtained from relation (6.10) of Ref. 12 for $p(r,\varphi,\varphi',\varphi'')$ for $Q = 0$, by integration with respect to r, φ and φ', between 0 and ∞, 0 and 2π and $-\infty$ and $+\infty$, respectively, and in turn by integration with respect to φ'' between φ_1'' and ∞. Considerable simplification is required to obtain (41).

For very large values of k the following approximation applies

$$P(|\varphi''| \geqq kb_2/b_0) \approx \frac{2}{\pi k}\left[1 + \ln\left(\frac{k}{2} + 1\right)\right] \tag{45}$$

where $\ln = \log_\epsilon$.

For a flat spectrum $W(\gamma) = W$ of bandwidth $\hat{\gamma}$

$$a = 9/5 \qquad \text{and} \qquad b_2/b_0 = \hat{\gamma}^2/3. \tag{46}$$

For a Gaussian power spectrum (18)

$$a = 3 \qquad \text{and} \qquad b_2/b_0 = \sigma^2. \tag{47}$$

The quantity $(b_2/b_0)^{\frac{1}{2}}$ is the rms frequency of the power spectrum and b_2/b_0 is the "variance."

The probability distribution (41) as obtained by numerical integration is shown in Tables II and III for flat and Gaussian power spectra. For large values of k, approximation (45) is shown in parentheses. These probability distributions are shown in Fig. 9.

III. TRANSMITTANCE VARIATIONS WITH FREQUENCY

3.1 *General*

In the previous section a sufficiently narrow signal band spectrum was assumed such that amplitude and phase distortion over the narrow band could be neglected. In this case it was necessary to consider time fluctuations in the transmittance over a pulse duration T that would be relatively long owing to the narrow spectrum bandwidth.

The other extreme of wideband transmission will now be considered, in which the duration of a pulse would be short enough for fluctuations in transmittance over a pulse interval to be disregarded. In this case it becomes necessary to consider variations in the transmittance with frequency over the much greater signal spectrum band. The variations in the amplitude and phase characteristics with frequency will fluctuate with time, so that it becomes necessary to determine the resultant

TABLE II — PROBABILITY DISTRIBUTION $P(|\varphi''| > k\hat{\gamma}^2/3)$ FOR FLAT POWER SPECTRUM

$k = 0$	1	2	3	4	5	10	20	50	100
1	.538	.381	.321	.269	.238	.158	.100	.051	.031 (.03)

TABLE III — PROBABILITY DISTRIBUTION $P(|\varphi''| > k\sigma^2)$ FOR GAUSSIAN POWER SPECTRUM

$k = 0$	1	2	3	4	5	10	20	50	100
1	.595	.447	.369	.317	.280	.182	.113	.057	.033 (.03)

transmission impairments on the basis of certain probability distributions.

In a first approximation the departure from a constant amplitude vs frequency characteristic will be a characteristic with a linear slope, as indicated in Fig. 10, that will vary with time. Similarly the departure from a constant transmission delay over the channel band can be approxi-

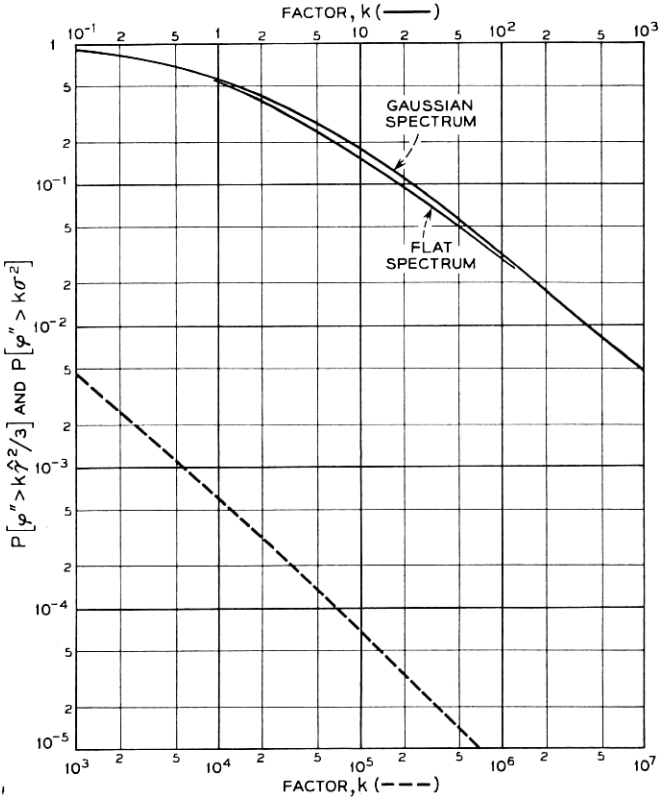

Fig. 9 — Probability that $\ddot{\varphi}$ exceeds "variance" of fading power spectrum by factor k for flat power spectrum with bandwidth $\hat{\gamma}$ and "variance" $\hat{\gamma}^2/3$ and for Gaussian power spectrum with "variance" σ^2.

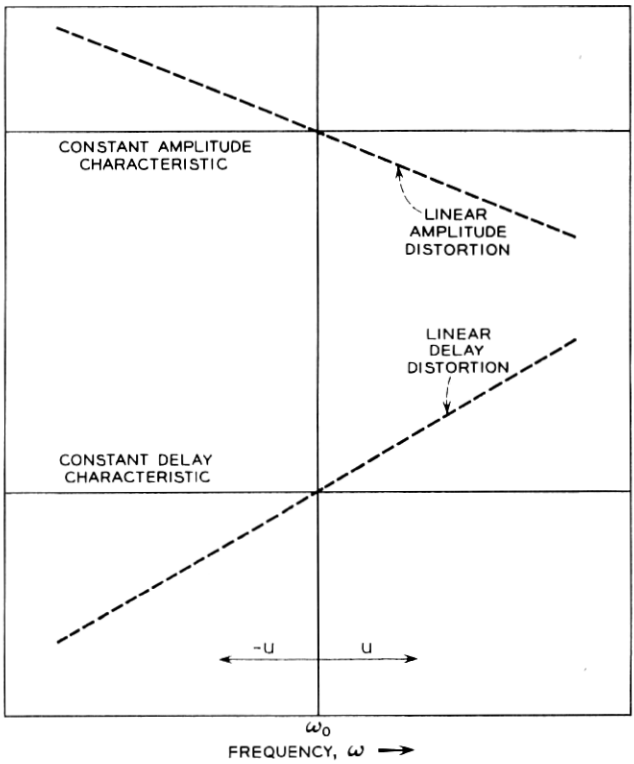

Fig. 10 — First approximations to random departures from constant amplitude and delay characteristics are represented by linear variations with frequency.

mated by a linear variation in transmission delay. The probability distributions of the slopes of these linear variations in the amplitude and delay characteristics are the same as for corresponding variations with time, with appropriate modification of the basic parameters, as discussed in the following.

3.2 *Amplitude and Phase Distributions*

Let the time t be fixed, and consider only variations in r and φ with the frequency ω of a number of transmitted sine waves.

Each sine wave could be regarded as a spectral component of a carrier pulse of very short duration with an essentially flat and continuous spectrum about the carrier frequency. In this case u rather than t is changed in expressions (5) and (6) for the two components $U(u,t)$ and $V(u,t)$. There will in this case be a particular variation with u for each

time t. When observations are made for a sufficiently large number of specified times, the resultant probability distribution of the amplitude and phase will be the same as discussed in Section 2.2 for variation in time for a given frequency u.

3.3 *Slope in Amplitude Characteristic* ($\dot{r}$)

At a particular time, the envelopes $r(u,t)$ of the received sine waves will vary with frequency u. The slope of the envelope will be designated $dr(u,t)/du = \dot{r}$. It will have a probability distribution as given by (30) for the time rate of change in $r(u,t)$. This probability distribution is

$$P(\,|\dot{r}| > |\dot{r}_1|\,) = P(\,|\dot{r}| \geqq k\dot{\bar{r}}) = \operatorname{erfc}(k/2^{\frac{1}{2}}) \tag{48}$$

where erfc is the error function complement and

$$\begin{aligned} k &= \dot{r}_1/\dot{\bar{r}} \\ \dot{\bar{r}} &= \text{rms value of } \dot{r} \\ &= [\tfrac{1}{2}(b_2 - b_1^2/b_0)]^{\frac{1}{2}} \end{aligned} \tag{49}$$

except that now

$$b_n = \int_0^\infty W(\delta)\delta^n \, d\delta \tag{50}$$

where $W(\delta)$ is the power spectrum given by (21). When $W(\delta)$ is given by (22), (50) gives $b_0 = \Psi(0)/\Delta$; $b_1 = \Psi(0)\Delta^2/2$; $b_3 = \Psi(0)\Delta^3/3$ and (49) yields

$$\dot{\bar{r}} = \bar{r}\Delta/6^{\frac{1}{2}} \tag{51}$$

where $\bar{r} = \Psi(0)^{\frac{1}{2}}$ is the rms amplitude of the envelope.

3.4 *Envelope Delay Distribution*

The envelope delay at a particular time t and frequency u is given by $\dot{\varphi} = d\varphi(u,t)/du$. The probability distribution of this delay $\dot{\varphi}$ is given by (36) or (38). Thus

$$\begin{aligned} P(\,|\dot{\varphi}| > |\dot{\varphi}_1|\,) &= P[\,|\dot{\varphi}| \geqq k(b_2/b_0)^{\frac{1}{2}}] \\ &= 1 - \frac{k}{\sqrt{1+k^2}} \end{aligned} \tag{52}$$

where as before

$$k = (b_0/b_2)^{\frac{1}{2}}\dot{\varphi}_1 \tag{53}$$

where b_0 and b_2 are given by (50).

For a flat power spectrum (22)

$$(b_2/b_0)^{\frac{1}{2}} = \Delta/3^{\frac{1}{2}} \approx 0.58\Delta. \tag{54}$$

3.5 *Distribution of Linear Delay Distortion*

The slope $\ddot{\varphi} = d\dot{\varphi}/du$ at a particular time represents linear delay distortion. The probability that $\ddot{\varphi}$ exceeds a specified value $\ddot{\varphi}_1$ is given by (41), or

$$\begin{aligned} P(|\ddot{\varphi}| > |\ddot{\varphi}_1|) &= F(|\ddot{\varphi}| \geqq kb_2/b_0) \\ &= 1 - \frac{2k}{\pi}\int_0^\infty \frac{dx}{(g(x) + k^2)g(x)} \\ &\quad - \frac{2}{\pi}\int_0^\infty \frac{\tan^{-1}(k/g^{\frac{1}{2}}(x))}{(1+x^2)^{\frac{3}{2}}}\,dx. \end{aligned} \tag{55}$$

For very large values of k (45) applies, or

$$P(|\ddot{\varphi}| \geqq kb_2/b_0) \approx \frac{2}{\pi k}\left[1 + \ln\left(\frac{k}{2} + 1\right)\right] \tag{56}$$

where now

$$k = b_0\ddot{\varphi}_1/b_2 \tag{57}$$

$$g(x) = (a - 1 + 4x^2)(1 + x^2) \tag{58}$$

$$a = b_0b_4/b_2^2 \tag{59}$$

and b_n is given by (50).

For a flat power spectrum (22)

$$b_2/b_0 = \Delta^2/3. \tag{60}$$

The probability distribution (55) as a function of k is given previously in Table II for a flat power spectrum and is shown in Fig. 9.

IV. ERRORS FROM TRANSMITTANCE VARIATIONS WITH FREQUENCY

4.1 *General*

As discussed later, the error probability in digital transmission over noisy channels with selective Rayleigh fading can be approximated by combining the probability of errors from three basic sources. One of these is errors from random noise determined in the presence of flat Rayleigh fading. The second source is errors from time variations in the transmittance, which is important at low transmission rates. The third

source is errors from transmittance variations with frequency, which becomes important at high transmission rates and puts an upper bound on the transmission rate for a specified error probability. In this section an approximate evaluation is made of errors on the latter account.

As a first approximation, the statistical properties of transmittance variations with frequency, ordinarily referred to as selective fading, can be represented by the probability distribution (48) of $\dot{r}$ and (55) of $(\ddot{\varphi})$. The first of these represents a linear slope on the amplitude vs frequency characteristics, and the second represents a linear variation in transmission delay. Errors will occur even in the absence of noise, when $\dot{r}$ or $\ddot{\varphi}$ exceeds certain maximum values. These maxima will depend on the spectrum of pulses in the absence of distortion, on the pattern of transmitted pulses and on the carrier modulation method. After these maximum values are determined, it is possible to determine the probability of encountering them with the aid of the probability distributions of $\dot{r}$ and $\ddot{\varphi}$ given in Section III.

4.2 *Carrier Pulse Transmission Characteristics*

It will be assumed that a carrier pulse of rectangular or other suitable envelope is applied at the transmitting end of a bandpass channel. The received pulse with carrier frequency ω_0 can then be written in the general form[13]

$$P_0(t) = \cos(\omega_0 t - \psi_0) R_0(t) + \sin(\omega_0 t - \psi_0) Q_0(t) \tag{61}$$

$$= \cos[\omega_0 t - \psi_0 - \varphi_0(t)] \bar{P}_0(t), \tag{62}$$

where

$$\bar{P}_0(t) = [R_0^2(t) + Q_0^2(t)]^{\frac{1}{2}}, \tag{63}$$

$$\varphi_0(t) = \tan^{-1}[Q_0(t)/R_0(t)], \tag{64}$$

$$R_0(t) = \bar{P}_0(t) \cos \varphi_0(t), \tag{65}$$

$$Q_0(t) = \bar{P}_0(t) \sin \varphi_0(t). \tag{66}$$

In the above relations R_0 and Q_0 are the in-phase and quadrature components of the received carrier pulse and $\bar{P}_0(t)$ the resultant envelope. The time t is taken with respect to a conveniently chosen origin, for example the midpoint of a pulse interval or the instant at which $R_0(t)$ or $\bar{P}_0(t)$ reaches a maximum value.

Let $S_0(u)$ be the spectrum of received pulses at the output of the receiving filter, i.e., at the detector input, and $\psi_0(u)$ the phase function

of the spectrum, as illustrated in Fig. 11. The functions $R_0(t)$ and $Q_0(t)$ are then given by[13]

$$R_0 = R_0^- + R_0^+, \qquad Q_0 = Q_0^- - Q_0^+,$$

$$R_0^- = \frac{1}{\pi}\int_0^{\omega_0} S_0(-u)\cos[ut + \Psi_0(-u)]\,du, \tag{67}$$

$$R_0^+ = \frac{1}{\pi}\int_0^{\infty} S_0(u)\cos[ut - \Psi_0(u)]\,du, \tag{68}$$

$$Q_0^- = \frac{1}{\pi}\int_0^{\omega_0} S_0(-u)\sin[ut + \Psi_0(-u)]\,du, \tag{69}$$

$$Q_0^+ = \frac{1}{\pi}\int_0^{\infty} S_0(u)\sin[ut - \Psi_0(u)]\,du. \tag{70}$$

The upper limit ω_0 can ordinarily be replaced by ∞, since $S_0(-\omega_0) = 0$.

Let $S(u)$ be the spectrum in the absence of amplitude distortion, and $A(u)$ the amplitude characteristic of the channel. The received spectrum is then, for a time invariant channel

$$S_0(u) = S(u)A(u). \tag{71}$$

4.3 *Ideal Pulse Spectra and Pulse Shapes*

In carrier pulse transmission over an ideal channel the sideband spectrum of carrier pulses at the detector input will be symmetrical

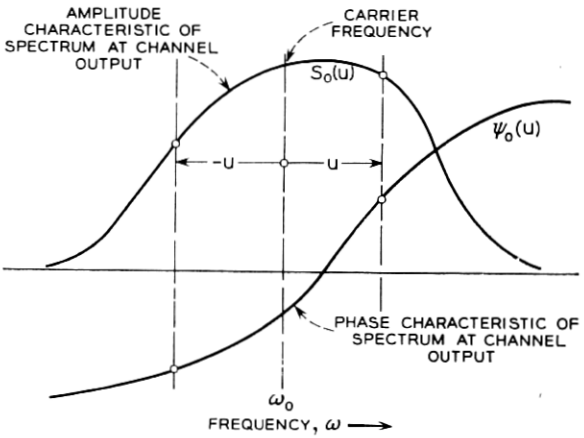

Fig. 11 — Amplitude and phase functions of pulse spectrum at channel output, i.e., detector input.

about the carrier frequency. As discussed elsewhere,[14] it is possible to realize optimum performance in binary transmission by AM, PM and FM with an infinite variety of pulse spectra at the detector input, with the general properties illustrated in Fig. 12. With all of these spectra, pulses can be transmitted without intersymbol interference at intervals

$$T = \pi/\Omega = 1/2B \tag{72}$$

where B is the mean bandwidth in cps to each side of the carrier frequency, as indicated in Fig. 12.

A desirable pulse spectrum in various respects is a raised cosine spectrum as illustrated in Fig. 13, given by

$$S(u) = S(-u) = \frac{\pi}{\Omega} \cos^2 \frac{\pi}{4} \frac{u}{\Omega}. \tag{73}$$

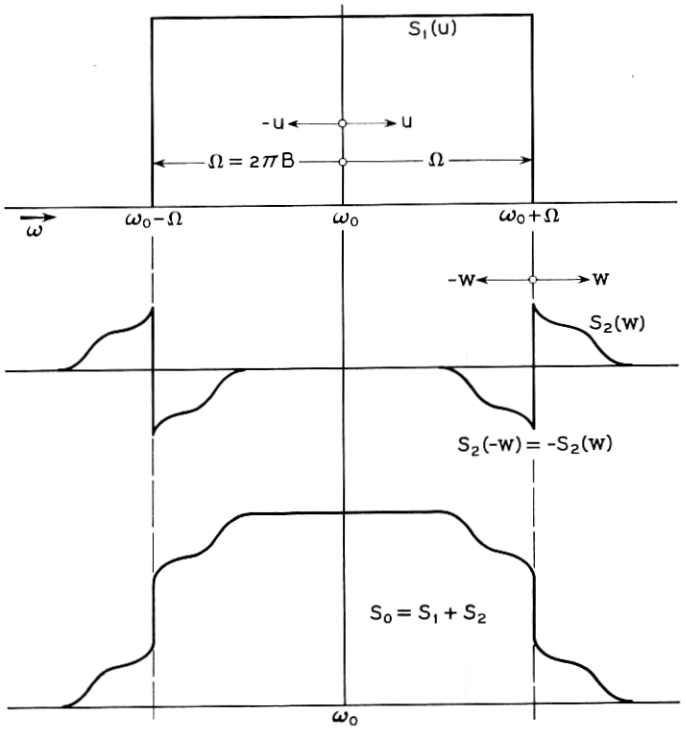

Fig. 12 — General properties of ideal spectra of carrier pulses at channel output (detector input) that permit pulse transmission without intersymbol interference at intervals $T = \pi/\Omega = 1/2B$.

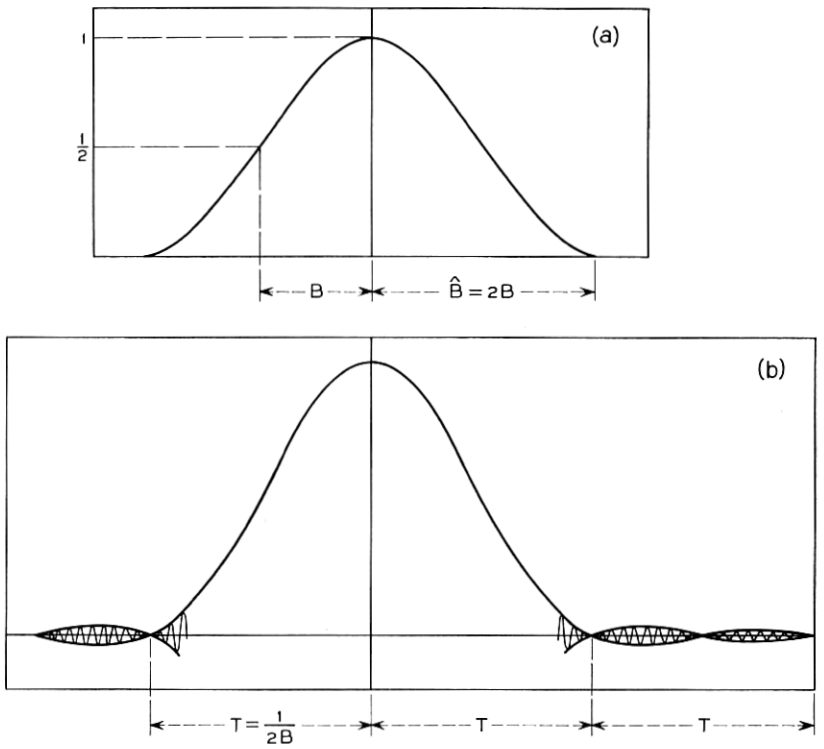

Fig. 13 — (a) Raised cosine bandpass pulse spectrum and (b) carrier pulse transmission characteristic, i.e., envelope of a carrier pulse.

The corresponding carrier pulse at the detector input as shown in Fig. 13 is given by

$$P_0(t) = \bar{P}_0(t) \cos (\omega_0 t - \varphi_0) \tag{74}$$

where

$$\bar{P}_0(t) = R_0(t) = \frac{\sin \Omega t}{\Omega t} \frac{\cos \Omega t}{1 - (\Omega t/\pi)^2}. \tag{75}$$

4.4 *Linear Variation in Amplitude Characteristic*

Let $\psi_0(u) = 0$ and

$$A(u) = 1 + cu \tag{76}$$

where c is a constant. In this case (71) becomes

$$S_0(u) = S(u)(1 + cu). \tag{77}$$

When the received spectrum in the absence of distortion has even symmetry about the carrier frequency ω_0, such that $S(-u) = S(u)$, (77) in (67) to (70) gives

$$R_0(t) = \frac{2}{\pi}\int_0^\infty S(u)\cos \omega t\, du \tag{78}$$

$$Q_0(t) = -\frac{c^2}{\pi}\int_0^\infty uS(u)\sin ut\, du \tag{79}$$

$$= c\frac{d}{dt}R_0(t) = cR_0'(t). \tag{80}$$

In the case of a raised cosine spectrum, $R_0(t)$ is given by (75) and (80) yields

$$Q_0(t) = c2\Omega\frac{\cos 2\Omega t}{2\Omega t[1 - (2\Omega t/\pi)^2]} - c2\Omega\frac{\sin 2\Omega t}{(2\Omega t)^2[1 - (2\Omega t/\pi)^2]^2} \tag{81}$$

$$= 0 \quad \text{for} \quad t = 0. \tag{82}$$

At the first sampling points before and after $t = 0$, $t = \pm T = \pm(\pi/\Omega)$ and (81) yields

$$Q_0(\pm T) = \pm c\Omega/3\pi. \tag{83}$$

At the next sampling points $t = \pm 2T = \pm 2\pi/\Omega$

$$Q_0(\pm 2T) = \pm c\Omega/30\pi. \tag{84}$$

From (83) and (84) it appears that only the first sampling points $t = \pm T$ need to be considered in determining the effect of linear amplitude distortion.

4.5 *Probability of Errors from Linear Amplitude Distortion*

The rms amplitude of the component $Q_0(\pm T)$ is given by

$$\bar{Q}_0(\pm T) = \bar{c}\Omega/3\pi = \bar{c}\hat{B}/3 \tag{85}$$

where $\hat{B} = 2\Omega/2\pi$ and $\bar{c}$ is the rms amplitude of $\dot{r}$ as given by (51) or

$$\bar{c} = \dot{\bar{r}} = \bar{r}\Delta/6^{\frac{1}{2}}. \tag{86}$$

Thus (85) becomes

$$\bar{Q}_0(\pm T) = \bar{r}(\hat{B}\Delta/3\cdot 6^{\frac{1}{2}}). \tag{87}$$

The rms amplitude of $R_0(0)$ is $\bar{r}$. Hence

$$\bar{\eta} = \frac{\bar{Q}_0(T)}{\bar{R}_0(0)} = \frac{\hat{B}\Delta}{3 \cdot 6^{\frac{1}{2}}}. \tag{88}$$

This is the ratio of rms intersymbol interference at the first sampling points to the rms value of the peak pulse amplitude.

The probability of exceeding the above ratio by a factor k is, in accordance with (48)

$$P(\eta \geqq k\bar{\eta}) = \operatorname{erfc}(k/2^{\frac{1}{2}}). \tag{89}$$

The probability of error will depend on the carrier modulation method. In general, however, the approximate allowable peak value of η in the absence of noise is

$$\hat{\eta} \approx \tfrac{1}{2}. \tag{90}$$

The probability of exceeding this value, corresponding to $k = 3 \cdot 6^{\frac{1}{2}}/2\hat{B}\Delta$ is

$$P_e = \operatorname{erfc}(3 \cdot 3^{\frac{1}{2}}/2\hat{B}\Delta) \approx \operatorname{erfc}(2.6/\hat{B}\Delta). \tag{91}$$

This probability is much smaller than that resulting from a linear variation in delay over the transmission band. For example, if $\hat{B} = 10^6$ cps and $\Delta = 10^{-7}$ sec, $1/\hat{B}\Delta = 10^{-1}$ and $P_e = \operatorname{erfc}(26)$, which is negligible.

4.6 *Linear Variation in Envelope Delay*

It will be assumed that the phase distortion component is given by

$$\Psi_0(u) = cu^2, \tag{92}$$

which corresponds to a linear delay distortion given by

$$\Psi_0'(u) = 2cu. \tag{93}$$

In this case expressions (67) to (70) give for a raised cosine spectrum

$$R_0(-t) = R_0(t) = \frac{4}{\pi}\int_0^{\pi/2} \cos^2 x \cos \alpha x \cos bx^2 \, dx \tag{94}$$

$$Q_0(-t) = Q_0(t) = \frac{4}{\pi}\int_0^{\pi/2} \cos^2 x \cos \alpha x \sin bx^2 \, dx, \tag{95}$$

where

$$a = 4(t/T), \qquad b = (4/\pi)(d/T); \qquad T = (1/\hat{B})$$

in which the delay d is defined as in Fig. 14.

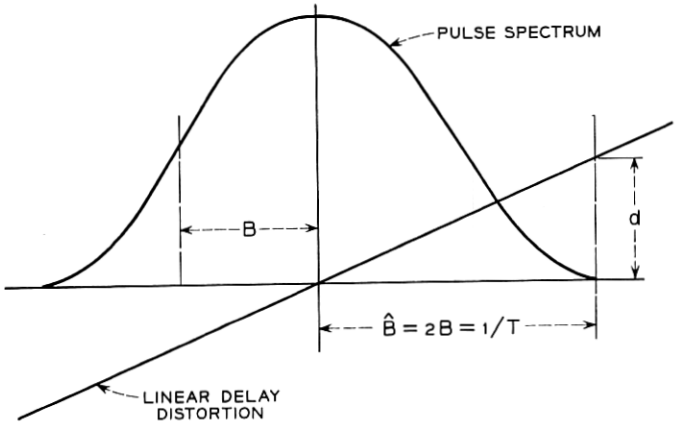

Fig. 14 — Raised cosine pulse spectrum with linear delay distortion.

The above integrals have been evaluated by numerical integration and are tabulated elsewhere.[13] The functions $R_0(t)$ and $Q_0(t)$ are shown in Fig. 15, as a function of $t/T = t\hat{B}$ for various values of $d/T = d\hat{B}$. The phase has been adjusted to 0 at $t = 0$, hence the notation R_{00} and Q_{00}.

4.7 *Maximum Tolerable Linear Delay Distortion*

Intersymbol interference at sampling points owing to linear delay distortion is significantly greater than that resulting from a linear slope in the amplitude characteristic. Moreover, pulse patterns that cause maximum intersymbol interference with linear delay distortion will not give rise to intersymbol interference from a linear slope in the amplitude characteristic, and conversely. For this reason it suffices to consider the more important component, i.e., linear delay distortion.

The reduction in tolerable noise power owing to linear delay distortion has been determined elsewhere[13] for binary AM with envelope detection, binary PM with synchronous detection, and binary FM with frequency discriminator detection. For these methods the reduction in noise margin is shown in Fig. 16 as a function of the parameter $\lambda = d/T = d \cdot \hat{B}$. In the same figure is shown the reduction in noise margin for two-phase and four-phase modulation, with differential phase detection as determined by methods similar to those for the other modulation methods in the above reference. These methods essentially consist in determining the maximum intersymbol interference that can be encountered, considering the pulse shapes shown in Fig. 15 and all possible pulse patterns over the number of pulse intervals that contribute

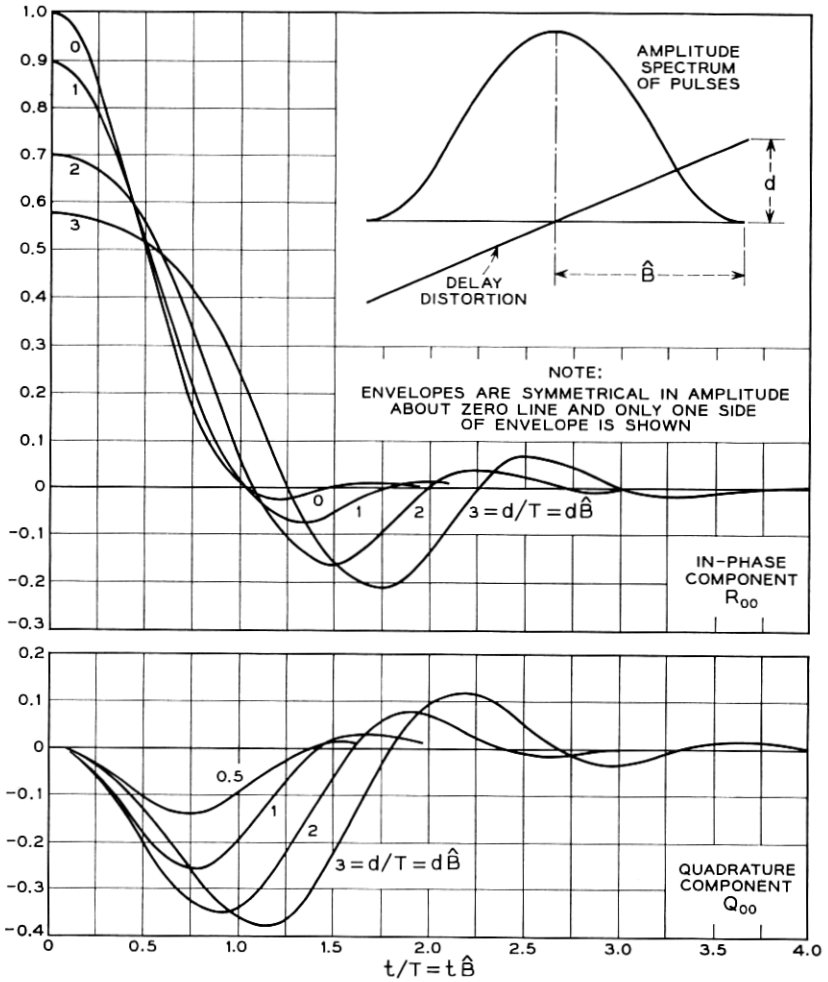

Fig. 15 — Carrier pulse transmission characteristics for raised cosine pulse spectrum and linear delay distortion. For negative values of $t/T = t \cdot \hat{B}$ the characteristics are the same as shown for positive values.

significantly to intersymbol interference. Exact analytic determination of the maximum impairments does not appear feasible, and it becomes necessary to resort to trials for selection of the worst condition. It should be noted that with binary PM with differential phase detection the optimum threshold level differs from zero owing to a bias component in the demodulator output.[13] The curve in Fig. 16 and the analysis that follows assume automatic adjustment to the optimum threshold level,

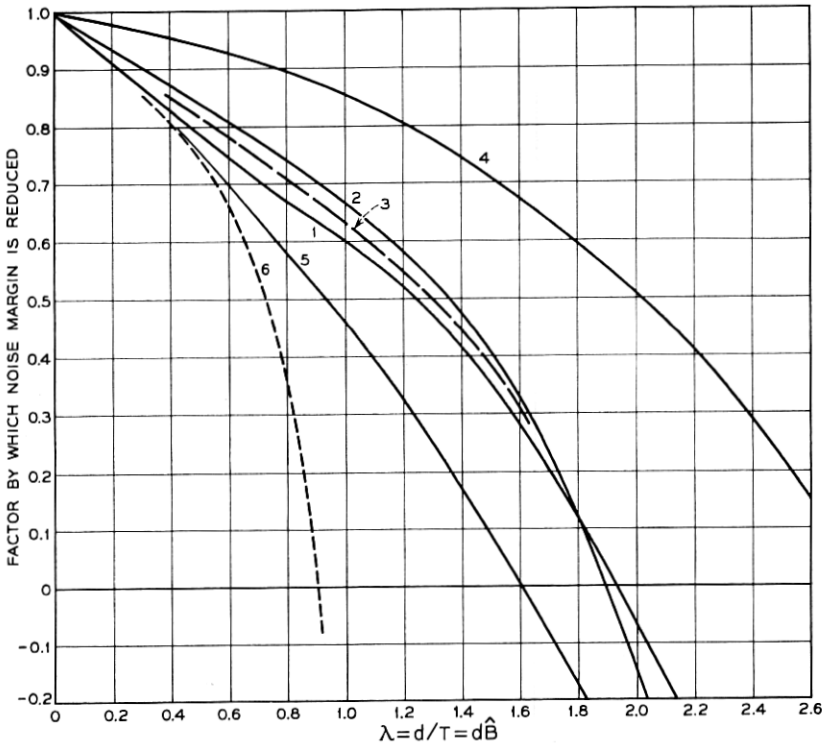

Fig. 16 — Maximum reduction in noise margin owing to linear delay distortion: 1, binary AM with envelope detection; 2, binary FM with frequency discriminator detection; 3, binary PM with differential phase detection; 4, binary PM with synchronous detection; 5, four-phase modulation with synchronous detection; 6, four-phase modulation with differential phase detection.

and a significantly greater error probability would be encountered with zero threshold level.

It will be noted that the noise margin is reduced to zero for certain values λ_0 of λ. These values apply for certain combinations of baseband pulses in about four pulse positions. The probability of this and other pulse patterns must be considered in evaluating error probability as discussed below.

4.8 *Probability of Errors from Linear Delay Distortion*

As λ is increased slightly above the value λ_0 mentioned above, intersymbol interference increases rapidly. Thus errors will occur for a value λ_e of λ only slightly greater than λ_0, for certain combinations of two

pulses, occurring at times $-T$ and $+T$ relative to the sampling instant $t = 0$. There are four possible combinations of these two pulses. For one of these (say 1, 1), an error will occur if $\lambda \geqq \lambda_e$. For another (say $-1, -1$), an error will occur if $\lambda \leqq -\lambda_e$. For the other combinations $(-1, 1)$ and $(1, -1)$, intersymbol interference will cancel so that the probability of error is zero. The probability of error is thus

$$\begin{aligned} P_e &= \tfrac{1}{2}(\tfrac{1}{4} + \tfrac{1}{4})P(\,|\lambda| \geqq |\lambda_e|\,) \\ &= \tfrac{1}{4}P(\,|\lambda| \geqq |\lambda_e|\,) \end{aligned} \tag{96}$$

where $P(\,|\lambda| \geqq |\lambda_e|\,)$ is the probability that the absolute value of λ is greater than λ_e.

For a given value $\lambda_e = d_e\hat{B}$ the corresponding slope $\ddot{\varphi}$ of the linear delay distortion is

$$\begin{aligned} \ddot{\varphi}_e &= d_e/2\pi\hat{B} \\ &= \lambda_e/2\pi\hat{B}^2. \end{aligned} \tag{97}$$

The following relation applies

$$P(\,|\lambda| \geqq |\lambda_e|\,) = P(\,|\ddot{\varphi}| \geqq |\ddot{\varphi}_e|\,). \tag{98}$$

The probability distribution represented by the right-hand side of (98) is given by (55) with $\ddot{\varphi}_1 = \ddot{\varphi}_e$. For small probabilities (56) applies, so that in view of (96) and (98) the error probability is

$$\begin{aligned} P_e &= \tfrac{1}{4}P(\,|\ddot{\varphi}| \geqq |\ddot{\varphi}_e|\,) \\ &= \frac{1}{2\pi k_e}\left[1 + \ln\left(\frac{k_e}{2} + 1\right)\right] \end{aligned} \tag{99}$$

where

$$\begin{aligned} k_e &= 3\ddot{\varphi}_e/\Delta^2 \\ &= 3\lambda_e/2\pi\Delta^2\hat{B}^2. \end{aligned} \tag{100}$$

With (100) in (99)

$$P_e = \frac{\Delta^2\hat{B}^2}{3\lambda_e}\left[1 + \ln\left(1 + \frac{3\lambda_e}{4\pi\Delta^2\hat{B}^2}\right)\right]. \tag{101}$$

From Fig. 16 it will be noted that for binary AM and FM, and for binary PM with differential phase detection, $\lambda_0 \approx 1.8$. For these cases it appears a legitimate approximation to take $\lambda_e = 2$. On this premise the error probabilities given in Table IV are obtained for various values of the parameter $\Delta\hat{B}$.

TABLE IV — PROBABILITY OF ERRORS IN A DIGIT OWING TO LINEAR DELAY DISTORTION IN ABSENCE OF NOISE FOR BINARY AM, FM AND PM (WITH DIFFERENTIAL PHASE DETECTION)

$\Delta\hat{B} = 10^{-4}$	10^{-3}	10^{-2}	10^{-1}
3.1×10^{-8}	2.4×10^{-6}	1.6×10^{-4}	8×10^{-3}

The above error probabilities are shown in Fig. 17 as a function of $\Delta\hat{B}$. If, for example, $\Delta = 10^{-7}$ second and $\hat{B} = 10^{5}$ cps, then $\Delta\hat{B} = 10^{-2}$ and $P_e = 1.6 \times 10^{-4}$. Pulses could in this case be transmitted at a rate of 100,000 per second with a minimum error probability $P_e = 1.6 \times 10^{-4}$. In the presence of noise the error probability will be greater, as discussed in a later section.

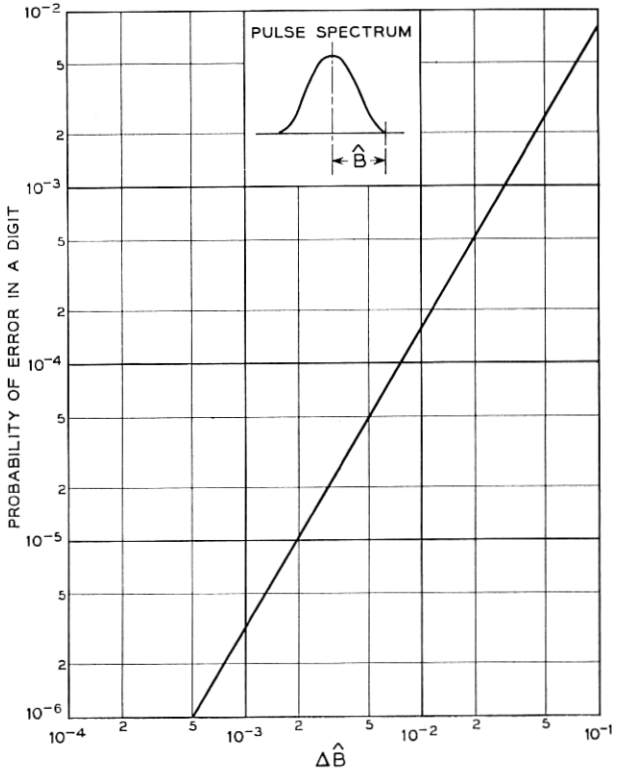

Fig. 17 — Error probability in binary AM, FM and PM owing to linear delay distortion for maximum departure Δ (seconds) from mean transmission delay.

The error probability with four-phase modulation and differential phase detection can be determined in a similar way. In this case $\lambda_0 \approx 0.9$ and $\lambda_e \approx 1$ in (101).

V. ERRORS FROM TRANSMITTANCE VARIATIONS WITH TIME

5.1 *General*

As mentioned in Section 4.1, transmittance variations with time is a second basic source of error in digital transmission. In transmission at low rates the bandwidth $\hat{B}$ of the pulse spectra will be narrow, so that fading can be regarded as constant over the spectrum band. Errors from selective fading, as considered in Section IV, can then be disregarded. On the other hand, the duration of a signal interval T may then be sufficiently long so that consideration must be given to random fluctuations in the amplitude, phase and frequency of the carrier between one signal interval and the next. Errors may occur owing to such fluctuations even in the absence of noise. The probability of errors in this account is evaluated here.

5.2 *Amplitude Variations*

The amplitude of a received wave will fluctuate with a Rayleigh distribution (10). Because of the great range of fluctuation, it is essential to provide automatic gain control at the receiver to prevent overloading and resultant adverse effects. Such gain control is activated by circuitry that integrates the received wave over a number of signal intervals T. With FM and PM only a few pulse intervals are required, for the reason that the received carrier wave is essentially independent of the pulse patterns. It is thus possible to provide effective gain control against rapid variations in the received carrier wave that occurs over a few signal intervals. Moreover, with FM and PM the distinction between marks and spaces is made by positive and negative deviations from zero threshold level in the detection process. This permits the use of limiters at the input to the detectors, to prevent the adverse effect of rapid fluctuations in the amplitude of the received carrier wave owing to fading. These advantages in applications to fading channels are not shared by AM, for reasons outlined below.

In binary AM or on-off carrier transmission, the received wave may be absent over a large number of consecutive signal intervals T. Hence automatic gain control must be activated by circuitry that integrates the received pulse train over a very large number of signal intervals T;

otherwise gain would be increased during long spaces, regardless of the fading condition. For this reason automatic gain control is inherently slow, in relation to the duration of a signal interval. It may thus be ineffective as applied to transmission at slow rates. With transmission at high rates, however, such that variations in the received wave owing to fading are inappreciable even over a large number of signal intervals, it may be possible to implement effective gain control.

At low transmission rates, such that fading is virtually constant over the band of the pulse spectrum, intersymbol interference can be made inappreciable. In this case it is possible to employ limiting prior to detection, and this method may then be more effective than automatic gain control, or could be used in conjunction with it. The limiter would slice the received wave at an appropriately selected level L. In the choice of the optimum slicing level it is necessary to consider the probability of errors during a mark owing to fading such that the received wave is less than L. In accordance with (10) this probability is

$$\begin{aligned} P(r \leqq L) &= 1 - \exp\,(-L^2/\bar{r}^2) \\ &\approx L^2/\bar{r}^2. \end{aligned} \tag{102}$$

A second consideration in the choice of L is the probability of errors owing to noise during a space, which is increased as L is reduced. The optimum threshold level considering both effects is determined in Section 6.9.

Owing to even small intersymbol interference, the use of a limiter as postulated above may be precluded in actual systems. For example, let L be 10 per cent of the rms signal amplitude $\bar{r}$, and let intersymbol interference be 5 per cent of L when the received signal is just equal to L. When the received signal is increased by a factor 20, intersymbol interference would be increased correspondingly and would be equal to L. Hence errors would occur even in the absence of noise. This is the inherent reason why limiting is generally ineffective as applied to binary AM. However, even if intersymbol interference could be disregarded, the error probability in the presence of noise will be greater than with binary PM or FM, as shown in Section 6.9.

5.3 *Carrier Frequency Variations*

In transmission over troposcatter links, random fluctuations will occur in the carrier frequency, which may be important from the standpoint of receiver implementation with any modulation method. Such fluctuations can be limited at the input to the IF filter with the aid of

signal-tracking oscillators for demodulation of the received radio frequency wave. The frequency of such oscillators may be controlled by feedback from the mixer output or from the detector output. The following expressions apply for the probability distribution of carrier frequency fluctuations without such frequency control at the receiver.

The probability distribution of frequency variations is given by (38). For a Gaussian fading power spectrum, the probability that the frequency variation $\varphi' = \Delta\omega$ exceeds $k\sigma$ is thus

$$P(\,|\,\Delta\omega\,|\,\geqq k\sigma) \approx (1/2k^2). \tag{103}$$

The equivalent fading bandwidth is in accordance with (19) $\bar{\gamma} \approx 1.25\sigma$. The probability that $\Delta\omega$ exceeds $k\bar{\gamma}$ is thus

$$P(\,|\,\Delta\omega\,|\,\geqq k\bar{\gamma}) \approx (1/3k^2). \tag{104}$$

Since σ and $\bar{\gamma}$ are nearly proportional to the carrier frequency, it follows that the frequency fluctuations encountered with a specified probability will be nearly proportional to the carrier frequency. By way of example let $\bar{\gamma} \approx 2$ radians/second or about 0.3 cps. The probability that the frequency fluctuation exceeds 30 cps is in this case obtained from (104) with $k = 100$ and is 3×10^{-5}. It appears that for bandwidths of the pulse spectra in excess of about 5000 cps, frequency fluctuations will not be important. However, for narrow band spectra the random frequency excursions may become excessive and give rise to errors, particularly with frequency modulation, as discussed below.

5.4 *Frequency Variations over a Signal Interval*

It will be assumed that the carrier frequency excursion is limited with the aid of a signal-tracking oscillator, or that a demodulation process is used in binary FM in which the change from mark to space is based on comparison of the frequencies in adjacent signal intervals of duration T. If the separation between mark and space frequencies is $2\Omega_{01}$, an error will occur if the frequency is changed by $+\Omega_{01}$ for a space and by $-\Omega_{01}$ for a mark.

From (41) it is possible to determine the probability of errors owing to frequency changes $\pm\Omega_{01}$ over a signal interval of duration T. The maximum permissible value of φ'' is determined from

$$\varphi_{\max}'' T = \pm\Omega_{01} \tag{105}$$

where the positive sign applies for a space and the negative sign for a mark.

With an ideal pulse spectrum the pulse interval is given by $T = \pi/\Omega$, so that (105) can be written

$$\varphi''_{\max} = \pm\Omega_{01}\Omega/\pi. \tag{106}$$

5.5 *Error Probability in Binary FM*

The error probability is in this case

$$P_e = \tfrac{1}{2}P(\,|\,\varphi''\,|\,\geqq\,|\,\varphi_{\max}''\,|\,) \tag{107}$$

where the factor $\frac{1}{2}$ occurs when the probability functions is defined in terms of the absolute values as in (41).

The parameter k defined by (42) in this case becomes

$$\begin{aligned} k_{\max} &= \varphi_{\max}''/\sigma^2 \\ &= \Omega_{01}\Omega/\pi\sigma^2. \end{aligned} \tag{108}$$

With frequency discriminator detection, $\Omega_{01} = \Omega$. For a raised cosine spectrum, $\hat{B} = 2B = \Omega/\pi$ and

$$k_{\max} = \pi\hat{B}^2/\sigma^2. \tag{109}$$

Employing (45), the probability (107) of an error becomes

$$P_e = \left(\frac{\sigma}{\pi\hat{B}}\right)^2\left[1 + \ln\left(1 + \frac{\pi\hat{B}^2}{2\sigma^2}\right)\right]. \tag{110}$$

In the above relation, σ is in radians/second while $\hat{B}$ is in cps. The equivalent fading bandwidth is, in accordance with (19), $\bar{\gamma} \approx 1.25\sigma$. The ratio of the maximum bandwidth $\hat{B}$ in cps to $\bar{\gamma}$ in cps is thus

$$\mu = \frac{\hat{B}}{\bar{\gamma}/2\pi} = \frac{2\pi\hat{B}}{1.25\sigma} \approx \frac{5\hat{B}}{\sigma}. \tag{111}$$

The probability of error (110) is given in Table V for various ratios μ. These error probabilities are shown in Fig. 18.

TABLE V — ERROR PROBABILITIES WITH BINARY FM FROM FLAT RAYLEIGH FADING IN ABSENCE OF NOISE

$\mu = 10$	100	1000	10000
$\hat{B}/\sigma = 2$	20	200	2000
6×10^{-3}	9.3×10^{-5}	1.4×10^{-6}	1.8×10^{-8}

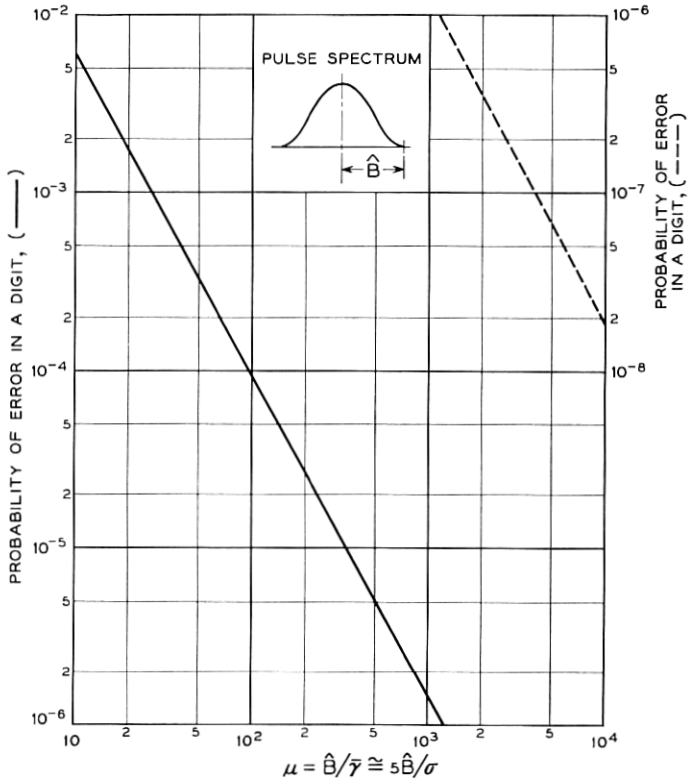

Fig. 18 — Error probability in binary FM in absence of noise, owing to frequency variations over a pulse interval T resulting from flat Rayleigh fading.

5.6 *Phase Variations over a Signal Interval*

The probability density of the carrier phase is $1/2\pi$, such that any phase may be encountered unless the carrier phase wander is limited by phase tracking oscillators in the demodulation process. In a digital phase modulation system where appreciable phase wander may be expected, the preferable demodulation method is differential phase detection. With this method the phase error will be limited to that encountered over a signal interval T.

From (36) it is possible to determine the probability of an error for a given maximum tolerable phase change θ over an interval T. For $k \gg 1$ the following relation applies

$$P(|\varphi'| \geqq |\varphi_1'|) = \frac{1}{2k^2} \tag{112}$$

$$= \frac{b_2}{2b_0}\frac{T^2}{\theta^2}. \tag{113}$$

With a Gaussian fading power spectrum (40) applies and

$$P[|\varphi'| \geqq (\varphi_1')] = (\sigma^2T^2/2\theta^2). \tag{114}$$

5.7 *Error Probabilities in PM*

With two-phase modulation $\theta = \pm(\pi/2)$, while with four-phase modulation $\theta = \pm(\pi/4)$. Hence the probability of error with these methods as obtained from (114) is, for two-phase modulation

$$P_e \approx (2/\pi^2)\sigma^2T^2 \approx 0.2\sigma^2T^2 \tag{115}$$

and for four-phase modulation

$$P_e \approx (8/\pi^2)\sigma^2T^2 \approx 0.82\sigma^2T^2. \tag{116}$$

These expressions apply provided the signal duration is sufficiently short so that the change in phase is small and can be considered linear over the interval. More accurate expressions that do not involve this assumption have been derived by Voelcker[9] for the error probability. Thus, with two-phase modulation the error probability is actually

$$P_e = \tfrac{1}{2}[1 - \kappa(T)] \tag{117}$$

and with four-phase modulation

$$P_e = \frac{1}{2} - \frac{2}{\pi}\kappa(T)[2 - \kappa^2(T)]^{-\frac{1}{2}} \tan^{-1}\frac{\kappa(T)}{[2 - \kappa^2(T)]^{\frac{1}{2}}} \tag{118}$$

where $\kappa(T) = \kappa(\tau)$ for $\tau = T$, i.e., the autocorrelation function for each quadrature component as defined by (15).

For a Gaussian fading spectrum, $\kappa(T)$ as obtained from (17) is

$$\kappa(T) = \exp(-\sigma^2T^2/2). \tag{119}$$

For $\sigma T \ll 1$:

$$\kappa(T) \approx 1 - \sigma^2T^2/2. \tag{120}$$

With the latter approximation in (117) and (118), the error probability with two-phase modulation becomes

$$P_e \approx \tfrac{1}{4}\sigma^2T^2 = 0.25\sigma^2T^2 \tag{121}$$

and with four-phase modulation

$$P_e = \left(\frac{1}{2} + \frac{1}{\pi}\right)\sigma^2 T^2 \approx 0.82\sigma^2 T^2 \tag{122}$$

which are to be compared with (115) and (116), respectively. The somewhat greater inaccuracy with two-phase than with four-phase modulation comes about since the phase change $\pm(\pi/2)$ cannot be considered small as required for (114) to apply.

In the above relations T is the interval between phase changes, which is related to the bandwidth of the baseband pulse spectrum. With idealized spectra of the type shown in Fig. 12, the interval is

$$T = 1/2B \text{ (two-phase)} \tag{123}$$

$$= 1/4B \text{ (four-phase)} \tag{124}$$

where B is the equivalent mean bandwidth.

In the particular case of pulses with a raised cosine spectrum, the maximum bandwidth is

$$\hat{B} = 2B \tag{125}$$

so that

$$\begin{aligned} T &= 1/\hat{B} \text{ (two-phase)} \\ &= 1/2\hat{B} \text{ (four-phase).} \end{aligned} \tag{126}$$

In terms of the above bandwidth the error probabilities (115) and (116) are thus the same for both two-phase and four-phase modulation and are given by

$$P_e \approx 0.05(\sigma/B)^2 \tag{127}$$

$$\approx 0.2(\sigma/\hat{B})^2. \tag{128}$$

The above relations apply for any number of phases. For this reason the capacity of a noiseless channel could be increased indefinitely by increasing the number of phases. There will, however, be certain limitations in this respect owing to intersymbol interference, as in stable channels.

The above error probability is shown in Table VI for various values of $\hat{B}/\sigma$ and $\mu = 5\hat{B}/\sigma$, where μ is the ratio defined by (111). It will be noted that these error probabilities are somewhat smaller than with binary FM as given in Table V.

The above probabilities of an error in a single digit are shown in Fig. 19, as a function of μ.

TABLE VI — ERROR PROBABILITIES WITH DIFFERENTIAL PM FROM FLAT RAYLEIGH FADING IN ABSENCE OF NOISE

$\mu = 10$	100	1000	10000
$\hat{B}/\sigma = 2$	20	200	2000
2×10^{-3}	2×10^{-5}	2×10^{-7}	2×10^{-9}

As noted in Section 1.6, there will be a certain median value of $\bar{\gamma}$ and thus a certain median value of μ and corresponding median error probability. During certain intervals, the error probabilities will be significantly smaller or significantly greater than the median error probabilities.

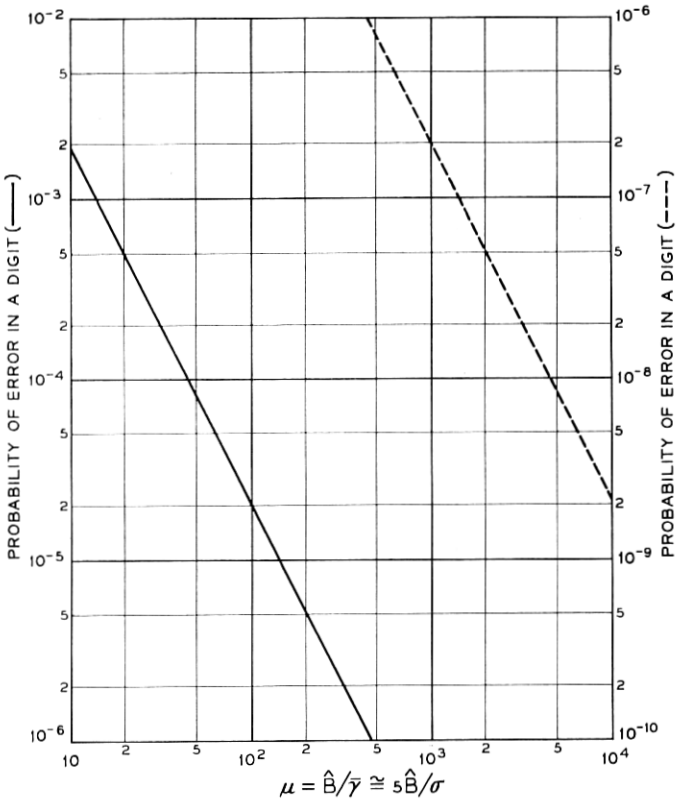

Fig. 19 — Error probability in binary PM with differential phase detection in absence of noise, owing to phase variations over pulse interval T resulting from flat Rayleigh fading.

VI. ERRORS FROM NOISE WITH FLAT RAYLEIGH FADING

6.1 *General*

As mentioned in Section 4.1, a third basic source of errors in troposcatter transmission is random noise. The probability of errors from noise depends on the modulation and detection methods and on their implementation. For optimum performance it is in the first place necessary to have appropriate pulse spectra such that intersymbol interference is avoided in transmission over ideal channels. Moreover, the error probability depends on the division of spectrum shaping between transmitting and receiving filters. The minimum error probabilities with various modulation and detection methods as quoted here are based on optimum design in the above and various other respects, such as accurate sampling of pulse trains. The probability of errors from noise in actual systems will be greater owing to various imperfections in implementation.

6.2 *Signal-to-Noise Ratios*

In carrier pulse transmission over an ideal channel, the sideband spectrum of the carrier pulses at the detector input will be symmetrical about the carrier frequency. As discussed elsewhere,[14] it is possible to realize optimum performance in binary transmission by AM, PM and FM with an infinite variety of pulse spectra at the detector input with the general properties discussed in Section 4.3.

The error probability in digital transmission over noisy channels is ordinarily specified in terms of the average signal-to-noise ratio at the input to the receiving filter that ordinarily precedes the detector. This signal-to-noise ratio is ordinarily taken as

$$\rho = S/N$$

S = average carrier power at detector input

N = average noise power in a flat band $B = 1/2T$ at input-to-receiving filter.

When S represents the average signal power in a fading channel, the designation $\bar{\rho} = S/N$ will be used in place of ρ.

The above reference band B is the minimum possible bandwidth in baseband pulse transmission without intersymbol interference. The minimum possible bandwidth in double sideband transmission as used in binary AM, PM and FM is $2B$.

The error probability as related to ρ will depend on the division of

spectrum shaping between transmitting filters and the receiving filter at the detector input. With optimum division, the error probability is the same as for transmission over a flat band B to each side of the carrier frequency.[14] Such a flat channel band is ordinarily assumed or implied in theoretical analyses, though not feasible in actual systems.

6.3 *Error Probabilities with Flat Rayleigh Fading*

Let r be the signal amplitude and $P_e^0(r)$ the error probability of errors owing to random noise in transmission over a stable channel with signal amplitude r. In the presence of fading, let the probability density of various signal amplitudes be $p(r)$. The error probability in transmission over fading channels is then

$$P_e = \int_0^\infty P_e^0(r)p(r)\,dr. \tag{129}$$

With Rayleigh fading the probability density $p(r)$ is the derivative of (27) with respect to r_1. With r in place of r_1 the probability density is

$$p(r) = (2r/\bar{r}^2)\exp(-r^2/\bar{r}^2) \tag{130}$$

$$= (r/S)\exp(r^2/2S) \tag{131}$$

where $S = \bar{r}^2/2$ is the average signal power.

6.4 *Binary PM with Synchronous Detection*

In binary PM, marks and spaces are transmitted by phase reversals. With ideal coherent or synchronous detection the error probability in transmission over a stable channel is

$$P_e^0 = \tfrac{1}{2}\operatorname{erfc}(\rho/2)^{\frac{1}{2}}. \tag{132}$$

The error probability with Rayleigh fading as obtained from (129) is, in this case[7,9]

$$P_e = \frac{1}{2}\left[1 - \left(\frac{\bar{\rho}}{\bar{\rho}+1}\right)^{\frac{1}{2}}\right] \approx \frac{1}{4\bar{\rho}} \tag{133}$$

where $\bar{\rho} = S/N$ = ratio of average received signal power with Rayleigh fading to average noise power as previously defined.

6.5 *Binary PM with Differential Phase Dection*

With binary PM and differential phase detection the error probability in transmission over a stable channel is[15]

$$P_e^0 = \tfrac{1}{2}e^{-\rho}. \tag{134}$$

The error probability with Rayleigh fading is, in this case[9]

$$P_e = 1/2(\bar{\rho} + 1). \tag{135}$$

6.6 *Binary FM with Dual Filter Detection*

With this method two receiving filters are used, centered on the space and mark frequencies ω_1 and ω_2, as indicated in Fig. 20, with sufficient separation to avoid mutual interference between the space and mark channels. Complementary binary amplitude modulation is used at the two carrier frequencies, and the two baseband filter outputs are combined with reversal in the polarity of one.

The error probability in transmission over stable channels with coherent detection is[16]

$$P_e^{\,0} = \tfrac{1}{2} \operatorname{erfc} (\rho^{\frac{1}{2}}/2) \tag{136}$$

and with noncoherent detection is[16]

$$P_e^{\,0} = \tfrac{1}{2} \exp (-\rho/2). \tag{137}$$

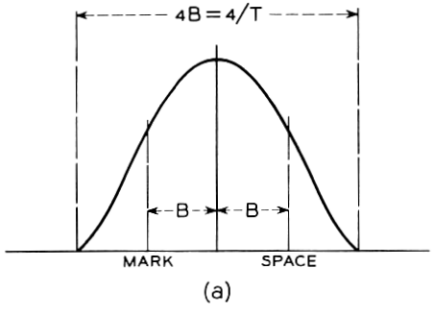

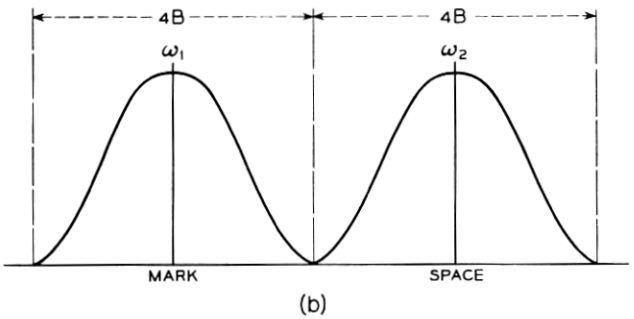

Fig. 20 — Comparison of channel bandwidth requirements in binary FM with (a) frequency discriminator detection and (b) dual filter detection.

Comparison of (136) with (132) shows that the error probability P_e with Rayleigh fading is obtained by replacing in (133) $\bar{\rho}$ with $\bar{\rho}/2$. This yields for coherent detection

$$P_e = \frac{1}{2}\left[1 - \left(\frac{\rho}{\bar{\rho}/2}\right)^{\frac{1}{2}}\right] \approx \frac{1}{2\bar{\rho}}. \tag{138}$$

Comparison of (137) with (134) shows that P_e is obtained by replacing in (135) $\bar{\rho}$ with $\bar{\rho}/2$, in which case, for noncoherent detection

$$P_e = 1/(\bar{\rho} + 2). \tag{139}$$

6.7 *Binary FM with Frequency Discriminator Detection*

With this method a single receiving filter is used, with space and mark frequencies as indicated in Fig. 20. Pulse transmission without intersymbol interference over a channel of the same bandwidth as required for double-sideband AM is in this case possible for certain ideal amplitude and phase characteristics of the channels, as shown elsewhere.[14]

The error probabilities in the absence of fading depends on the characteristics of the bandpass channel filters and the post-detection low-pass filter, and are difficult to determine exactly. Approximate evaluations[14] indicate that for a given error probability, about 4 db greater signal-to-noise ratio would be required than for binary PM with coherent detection, when no post-detection low-pass filter is used. Recent exact evaluations by Bennett and Salz,[17] indicate 3 to 4 db increase in the required signal-to-noise ratio over a variety of filter shapes. With an optimum post-detection low-pass filter, a small improvement may be realized, such that about 3 db increase over binary PM with coherent detection would be expected. On this basis it appears that the error probability will be virtually the same as for binary FM with dual filter coherent detection, such that the principal advantage over the latter method is a two-fold reduction in bandwidth.

6.8 *Binary AM with Ideal Gain Control*

It will be assumed that the receiver can be implemented with ideal automatic gain control, such that the output in the presence of a mark would have a fixed level l and in the presence of a space would be zero. This condition can be approached at sufficiently high transmission rates, such that the received wave prior to gain control changes insignificantly over a large number of pulse intervals of duration T. Under this condition the fading bandwidth is negligible relative to the bandwidth of the baseband pulse spectrum.

On the above premise and with ideal coherent (or synchronous) detection, the optimum threshold level for decision between marks and spaces would be $l/2$. The tolerable peak noise amplitude before an error occurs would be $l/2$, as compared with l for binary PM, resulting in 6 db reduction in noise margin. On the other hand, the average transmitter power is 3 db less than with binary PM. Hence this method would have a 3 db disadvantage compared to binary PM with synchronous detection.

Accordingly, (132) would be replaced by

$$P_e^{\,0} = \tfrac{1}{2} \operatorname{erfc} (\rho/4)^{\frac{1}{2}} \tag{140}$$

and (133) would be replaced by

$$P_e = \frac{1}{2}\left[1 - \left(\frac{\bar{\rho}}{\bar{\rho} + 2}\right)^{\frac{1}{2}}\right]. \tag{141}$$

The above relations are the same as (136) and (138) for binary FM with dual filter coherent detection, and (141) is virtually the same as (135) for binary PM with differential phase detection. Hence binary AM offers no advantage in signal-to-noise ratio even at sufficiently high transmission rates such that ideal gain control could be implemented.

6.9 *Binary AM with Optimum Fixed Threshold Detection*

At low transmission rates, such that the received wave can change appreciably over a few pulse intervals owing to fading, gain control cannot be effectively implemented, as discussed in Section 5.2. Without effective gain control, there will be a certain optimum threshold for distinction between marks and spaces. This optimum level and the corresponding signal-to-noise ratio is determined here on the premise that no gain control is used. This threshold level could be implemented by either a predetection or a postdetection limiter. Assume a probability $\frac{1}{2}$ of a mark being present; in the absence of noise, the probability of errors in marks is, in view of (102)

$$P_e(r \leqq L) = \tfrac{1}{2}[1 - \exp(-L^2/2S)] \tag{142}$$

where L is the threshold level. In the presence of noise the error probability will be only slightly greater than (142).

A second consideration in the choice of L is the probability of errors during a space. This error probability is obtained from (137) with $\rho = L^2/N$ and is

$$P_e(n \geqq L) = \tfrac{1}{2} \exp(-L^2/2N) \tag{143}$$

where n is the instantaneous noise amplitude and N the average noise power.

The combined error probability is

$$P_e = \tfrac{1}{2}[1 - \exp(-\mu/2) + \exp(-\bar{\rho}\mu/2)] \tag{144}$$

where

$$\mu = L^2/S; \qquad \bar{\rho} = S/N. \tag{145}$$

The optimum L or μ is obtained from the condition $dP_e/d\mu = 0$. This yields the following relation for the optimum value μ_0

$$\exp(-\mu_0/2) = \bar{\rho}\exp(-\bar{\rho}\mu_0/2) \tag{146}$$

or

$$\mu_0 = \frac{2\ln\bar{\rho}}{\bar{\rho} - 1} = \frac{4.606\log_{10}\bar{\rho}}{\bar{\rho} - 1}. \tag{147}$$

In practicable systems $\bar{\rho} \gg 1$, in the order of 100 or more, and $\mu_0 \ll 1$. With (147) in (144), the following approximation is obtained for the minimum error probability

$$P_{e,\min} \approx \frac{1}{2}\left[\frac{\ln\bar{\rho}}{\bar{\rho} - 1} + \exp(-\ln\bar{\rho})\right]. \tag{148}$$

The above error probability is significantly greater than with binary PM or FM. The error probability (148) is thus greater than for binary FM with dual filter coherent detection by a factor of at least $\ln\bar{\rho}$. For $\bar{\rho} = 1000$ (30 db) this factor is about $\ln\bar{\rho} \approx 7$. Hence about 10 $\log_{10} 7 \approx 8.5$ db greater average signal power would be required than with binary FM. This assumes that excessive intersymbol interference is avoided, which may not be feasible for reasons mentioned in Section 5.2. Since it is evident that binary AM is at a considerable disadvantage in signal-to-noise ratio as compared to binary PM and FM, it will not be considered further herein.

6.10 *Combined Rayleigh and Slow Log-Normal Fading*

In the previous determination of error probabilities, rapid Rayleigh fading was assumed, with a fixed mean signal-to-noise ratio $\bar{\rho}$ over the interval under consideration. It will now be assumed that in this interval there is a slow log-normal variation in path loss and thus in signal-to-noise ratio at the receiver, in conjunction with rapid Rayleigh fading.

Let P_e be the error probability with Rayleigh fading as previously

related to the mean signal-to-noise ratio $\bar{\rho} = \bar{s}^2/\bar{n}^2$, where $\bar{s}$ is the rms signal amplitude and $\bar{n}$ the rms noise amplitude. If $p(\bar{s})$ is the probability density of the rms amplitudes with slow fading, the probability of error in an interval during which the rms amplitude exceeds $\bar{s}_1$ is

$$P_{e,1} = \int_{\bar{s}_1}^{\infty} P_e(\bar{s}) p(\bar{s})\, d\bar{s}. \tag{149}$$

For $\bar{\rho} \gg 1$, the expression for $P_e(\bar{s})$ is of the general form

$$P_e(\bar{s}) \approx c/\bar{\rho} = \frac{c}{\bar{s}^2/\bar{n}^2}. \tag{150}$$

For binary PM with differential phase detection and for binary PM with coherent dual filter detection, $c = \frac{1}{2}$.

The probability density $p(\bar{s})$ is given by (12), or in the present notation

$$p(\bar{s}) = \frac{1}{\sqrt{2\pi}} \frac{1}{\sigma \bar{s}} \exp\left[-(\ln \bar{s}/\bar{s}_0)^2/2\sigma^2\right] \tag{151}$$

where $\bar{s}_0$ is the median rms amplitude and σ is the standard deviation of the fluctuation in $\bar{s}$.

With (150) and (151) in (144)

$$P_{e,1} = c \frac{1}{\sqrt{2\pi}} \frac{1}{\sigma} \int_{\bar{s}_1}^{\infty} \frac{1}{\bar{s}^2/\bar{n}^2} \frac{1}{\bar{s}} \exp\left[-(\ln \bar{s}/\bar{s}_0)^2/2\sigma^2\right] d\bar{s} \tag{152}$$

$$= \frac{c}{2} \frac{1}{\sqrt{2\pi}} \int_{\rho_1}^{\infty} \frac{1}{\rho^2} \exp\left[-(\tfrac{1}{2} \ln \rho/\rho_0)^2/2\sigma^2\right] d\rho \tag{153}$$

where $\rho_0 = \bar{s}_0^2/\bar{n}^2$ on $\rho_1 = \bar{s}_1^2/\bar{n}^2$.

Solution of (153) yields the relation

$$P_{e,1} = P_e \cdot \eta(\sigma, \kappa) \tag{154}$$

where

$$\kappa = \rho_1/\rho_0 \tag{155}$$

and

$$\eta(\sigma, \kappa) = \tfrac{1}{2} \exp(2\sigma^2) \operatorname{erfc}\left\{\frac{1}{\sqrt{8}\sigma}\left[4\sigma^2 + \ln \kappa\right]\right\}. \tag{156}$$

For $\rho_1 = 0$, $\ln \kappa = -\infty$ and $\operatorname{erfc}(-\infty) = 2$. Hence for this case

$$\eta = \exp(2\sigma^2). \tag{157}$$

This is the factor by which the error probability taken over a long interval is greater than without a log-normal variation in signal-to-noise ratio and only rapid Rayleigh fading.

Instead of modifying the error probability as above, an alternative method is to use an equivalent mean signal-to-noise ratio $\bar{\rho}_e$ that is smaller than $\bar{\rho}$ by the factor $\exp(-2\sigma^2)$. Thus

$$\bar{\rho}_e = \bar{\rho} \exp(-2\sigma^2). \tag{158}$$

When $\bar{\rho}_e$, $\bar{\rho}$ and σ are all expressed in db, expression (158) can alternatively be written

$$\bar{\rho}_{e,db} = \bar{\rho}_{db} - \sigma_{db}^2/8.69. \tag{159}$$

For example, with a representative value $\sigma_{db} = 8$ db, the last term in (159) is 7.4 db. Thus the charts in the later Figs. 21 and 22 apply when $\bar{\rho}$ is taken 7.4 db less than the median signal-to-noise ratios with log-normal fading.

VII. COMBINED ERROR PROBABILITY

7.1 *General*

In Sections IV to VI, three basic sources of errors in digital transmission over troposcatter links were discussed, and expressions were given for the probability of error from each of these sources in the absence of the others. In a first approximation, the error probability considering all three sources can be evaluated by taking the sum of the three error probabilities. Approximate expressions are given here for the resultant error probabilities, together with charts that facilitate determination of error probability as a function of the binary pulse transmission rate, when the basic system parameters are known. These are the average signal-to-noise ratio $\bar{\rho}$, the mean fading bandwidth $\bar{\gamma}$, and the maximum departure Δ from the mean transmission delay. The error probability for a given transmission rate can be reduced by various means that may or may not entail an increase in total transmitter power or bandwidth or both. For a given total transmitter power and bandwidth, the most effective means to this end is diversity transmission over independently fading paths, as discussed briefly herein.

7.2 *Combined Error Probability*

As a first approximation, the error probability is given by

$$P_e \approx P_e^{(1)} + P_e^{(2)} + P_e^{(3)} \tag{160}$$

where

$P_e^{(1)}$ = probability of errors in the absence of noise owing to intersymbol interference caused by frequency selective Rayleigh fading (Section IV)

$P_e^{(2)}$ = probability of errors in the absence of noise owing to random variations in carrier phase or frequency (Section V)

$P_e^{(3)}$ = probability or error owing to random noise with nonselective Rayleigh fading (Section VI).

As will be evident from the preceding discussion, and from charts that follow, $P_e^{(1)}$ can be disregarded when $P_e^{(2)}$ must be considered, and conversely, for error probabilities $P_e^{(3)}$ in the range of practical interest. Hence in actual applications (160) will take one of the following forms

$$P_e \approx P_e^{(1)} + P_e^{(3)} \tag{161}$$

$$P_e \approx P_e^{(2)} + P_e^{(3)}. \tag{162}$$

In addition, there are intermediate cases in which $P_e \approx P_e^{(3)}$.

In an exact determination of the error probability (161) it is necessary to consider the net effect of random intersymbol interference on the probability of errors owing to random noise, and similarly an exact determination of the error probability (162) the probability distribution of random phase deviations is involved. Intersymbol interference at a particular sampling instant may reduce or increase the tolerance to noise, and the net effect considering all pulse patterns may be such that (161) is a legitimate approximation. Similarly, random fluctuations in the slope of the phase characteristic may decrease or increase the tolerance to noise at a particular sampling instant, and the net effect considering all sampling instants may be such that (162) is a valid approximation. This is evidenced by the following exact relation derived by Voelcker[9] in place of (162) for binary PM with differential phase detection

$$P_e = [\bar{\rho}/(\bar{\rho} + 1)]P_e^{(2)} + P_e^{(3)}. \tag{163}$$

Since $\bar{\rho}$ would ordinarily exceed 100 (20 db), it follows that in this case (162) is a very good approximation to (163).

The exact error probability (161) depends on the probability distribution of phase distortion in conjunction with the probability distribution of intersymbol interference, which involves consideration of all pulse patterns. The combined probability distribution, and in turn the exact error probability, would be very difficult to determine, and hence the inaccuracy involved in (161) cannot readily be assessed. However, if

the probability distribution of intersymbol interference were the same as that of the reduction in tolerance to noise owing to random fluctuations in the slope of the phase characteristic, the inaccuracy in (161) would be no greater than that indicated by (162) versus (163). In most engineering applications, substantially greater inaccuracy would be permissible in the estimation of error probability, such that (161) and hence (160) can be considered permissible approximations in the present context.

The above expression (160) is applied below to binary PM and FM.

7.3 *Binary PM with Differential Phase Detection*

For binary PM with differential phase detection $P_e^{(1)}$ is given by (101) with $\lambda_e = 2$ or

$$P_e^{(1)} = \frac{\Delta^2\hat{B}^2}{6}\left[1 + \ln\left(1 + \frac{3}{2\pi\Delta^2\hat{B}^2}\right)\right]. \tag{164}$$

This error probability is given in Table IV as a function of $\Delta\hat{B}$.

The error probability $P_e^{(2)}$ is obtained from (117), or approximation (121)

$$P_e^{(2)} = \tfrac{1}{2}[1 - \kappa(T)] \tag{165}$$

$$\approx 0.25(\sigma T)^2 \approx 0.06(\sigma/\hat{B})^2 \tag{166}$$

$$\approx 0.039(\bar{\gamma}/\hat{B})^2. \tag{167}$$

The error probability $P_e^{(3)}$ is given by (135) or

$$P_e^{(3)} = 1/2(\bar{\rho} + 1). \tag{168}$$

7.4 *Error Probability Charts for Binary PM*

In Fig. 21 are shown the error probabilities $P_e^{(1)}$, $P_e^{(2)}$ and $P_e^{(3)}$ as a function of the transmission rate, for a raised cosine spectrum. The error probability $P_e^{(1)}$ depends on the maximum deviation Δ from the mean transmission delay, and curves are shown for a number of values of Δ. The probability $P_e^{(2)}$ depends on the mean fading bandwidth $\bar{\gamma}$, and curves applying for several values of $\bar{\gamma}$ are shown. Finally, the error probability $P_e^{(3)}$ depends on $\bar{\rho}$, and is shown for a number of different values of $\bar{\rho}$.

By way of illustration, the combined error probability obtained from (170) is shown by the dashed line in Fig. 20 for the particular case in which $\Delta = 10^{-7}$ second, $\bar{\gamma} = 2$ cps and $\bar{\rho} = 10^4$ (40 db).

The error probability as a function of transmission rate shown by this dashed line could apply to a variety of tropospheric scatter links,

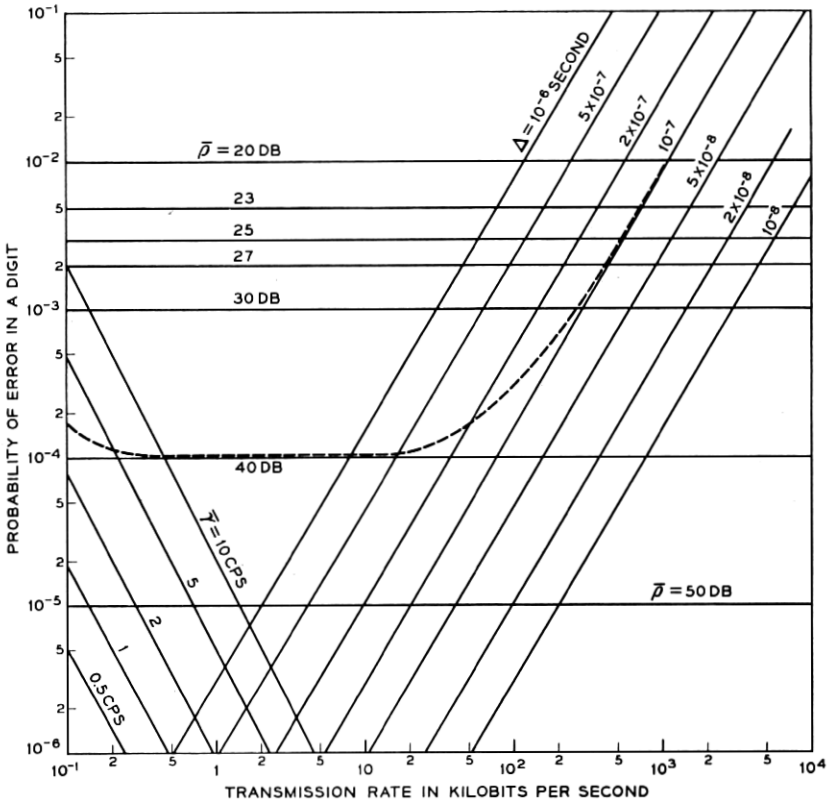

Fig. 21 — Probabilities of errors in binary PM with differential phase detection: 1, curves for various departures from mean delay show error probabilities in absence of noise owing to pulse distortion from selective fading; 2, curves for various mean fading bandwidths $\bar{\gamma}$ show error probabilities in absence of noise owing to random phase variations caused by flat fading; 3, curves for various mean signal-to-noise ratios $\bar{\rho}$ show error probabilities owing to noise for flat Rayleigh fading; 4, dashed curve shows approximate combined error probability for $\bar{\rho}$ = 40 db, $\Delta = 10^{-7}$ second, and $\bar{\gamma}$ = 2 cps.

since Δ depends on the length of the link and on the antenna beam angles. Moreover, $\bar{\rho}$ depends on the transmitter power, the length of the link, and the antenna beam angles. Hence, given values of Δ and $\bar{\rho}$ can be realized for a great variety of conditions.

7.5 *Binary FM with Frequency Discriminator Detection*

With frequency discriminator detection, the minimum required bandwidth for a given pulse transmission rate is the same as for binary PM, and half as great as that required with dual filter detection.

The error probability $P_e^{(1)}$ is in a first approximation the same as (161) for binary PM with differential phase detection. For the error probability $P_e^{(2)}$, approximation (110) applies, or

$$P_e^{(2)} = \left(\frac{\sigma}{\pi\hat{B}}\right)^2 \left[1 + \ln\left(1 + \frac{\pi\hat{B}^2}{2\sigma^2}\right)\right]. \tag{169}$$

This error probability is given in Table V as a function of $\hat{B}/\sigma$.

The probability of error owing to noise is, in a first approximation, the same as given by (139) for dual filter detection with coherent detection, or

$$P_e^{(3)} \approx 1/2\bar{\rho}. \tag{170}$$

7.6 *Error Probability Charts for Binary FM*

In Fig. 22 are shown the error probability $P_e^{(1)}$, $P_e^{(2)}$ and $P_e^{(3)}$ for binary FM as a function of the transmission rate. The curves apply for a raised cosine pulse spectrum, and the same basic parameters σ, $\bar{\gamma}$ and $\bar{\rho}$ as shown in Fig. 21 for binary PM. The error probability for the particular set of parameters previously assumed in Section 7.4 is shown by the dashed curve.

Comparison of the curves in Figs. 21 and 22 shows that the error probabilities are the same with both methods except at very low transmission rates. This applies only as a first approximation and with ideal implementation of both methods.

7.7 *Diversity Transmission Methods*

In diversity transmission, either space, frequency or time diversity can be used. The performance would be the same with these methods, and is an optimum when there is no correlation between the diversity paths. This entails adequate separation of receiving antennas in space diversity, adequate frequency separation in frequency diversity, or adequate time intervals between repetition of signals in time diversity.

With any one of the above three methods, different combining or decision procedures can be used at the receiver, as discussed in considerable detail by Brennan.[17] The optimum method from the standpoint of minimum required signal power for a specified error probability is known as "maximal ratio combining," in which the gain of the receiver in each path is made proportional to the input signal-to-noise ratio. This method is difficult to implement, and a simpler but somewhat less efficient method is "equal gain combining," in which the various receivers have equal gain and the demodulator baseband output are combined linearly.

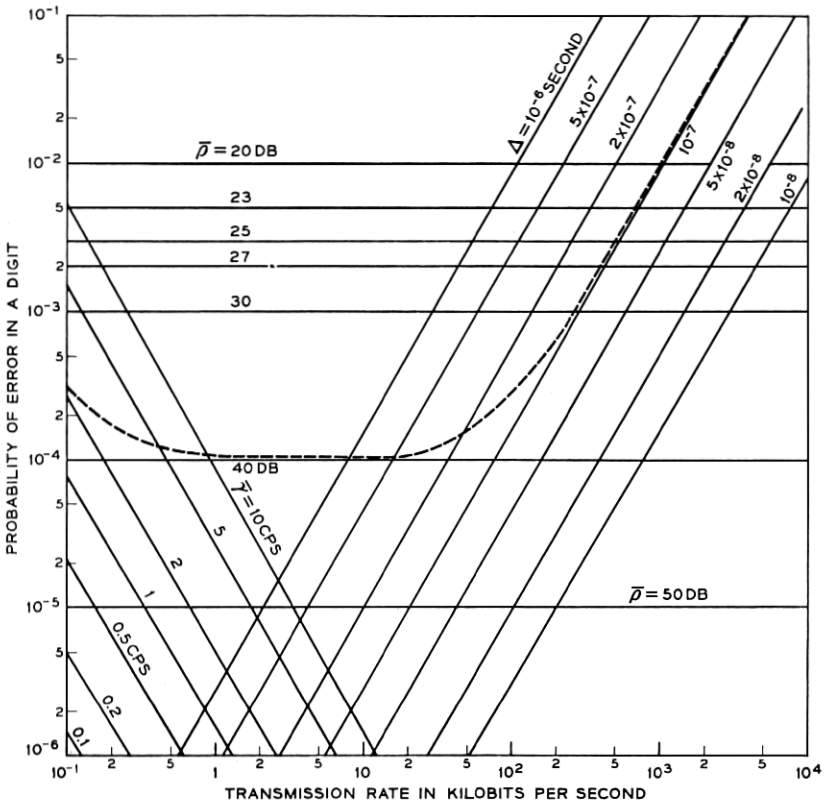

Fig. 22 — Probabilities of errors in binary FM with frequency discriminator detection: 1, curves for various departures Δ from mean delay show error probabilities in absence of noise owing to pulse distortion from selective fading; 2, curves for various mean fading bandwidths $\bar{\gamma}$ show error probabilities in absence of noise owing to random frequency variations caused by flat fading; 3, curves for various mean signal-to-noise ratios $\bar{\rho}$ at detector input show error probabilities owing to noise for flat Rayleigh fading; 4, dashed curve shows approximate combined error probability for $\bar{\rho}$ = 40 db, $\Delta = 10^{-7}$ second and $\bar{\gamma}$ = 2 cps.

This entails a demodulator in each diversity channel and common gain control of the various channels. The need for a demodulator in each diversity channel and common gain control is avoided with "selection diversity," in which the receiver having the largest signal is selected. Though this method is somewhat less efficient than equal gain combining, it has greater flexibility in that it can be used in conjunction with both linear and nonlinear modulation and detection methods, with path selection on the basis of predetection as well as post detection signals.

The principal diversity techniques would thus be space, frequency

or time diversity, in conjunction with "equal gain combining" or "selection diversity." The error reduction afforded by the two latter methods is discussed below.

7.8 *Error Probabilities with Equal Gain Diversity*

The error reduction afforded by equal gain diversity transmission has been determined by Pierce[8] for binary FM with coherent and noncoherent dual filter detection, on the premise of sufficiently slow flat Rayleigh fading, such that errors from noise alone need to be considered. For binary PM with differential phase detection, the error probability with equal gain diversity transmission has been determined by Voelcker,[9] considering both errors from noise [$P_e^{(3)}$] and errors from time variations in the transmittance [$P_e^{(2)}$]. Voelcker has also determined the error probability with dual diversity transmission for four-phase modulation with differential phase detection, considering errors from transmittance variations with time alone. For all of the above cases, the following approximation applies for the probability of single digit errors with dual diversity transmission over independently fading paths

$$P_{e,2} \approx 3P_{e,1}^2 \tag{171}$$

where $P_{e,1}$ is the error probability for transmission over a single path (no diversity). For four-phase modulation, Voelcker's more exact expression, when reduced to small error probabilities, gives a factor $4\pi(3 + \pi)/(2 + \pi)^2 \approx 3.13$ in place of 3 in (171).

The mechanism responsible for error reduction by diversity transmission in the above cases also applies to transmission over channels with selective fading when the errors are caused principally by intersymbol interference. With independently fading transmission paths there will be no correlation between intersymbol interference in the various channels, even though the signals are the same. Hence relation (171) would also be expected to apply for the combined error probability P_e given by (160).

For small error probabilities, the following approximate expression is given by Pierce[8] for the error probability owing to noise with flat Rayleigh fading for binary FM and multidiversity transmission

$$P_{e,m} \approx \frac{(2m-1)!}{m!\,(m-1)!} P_{e,1}^m \tag{172}$$

$$P_{e,2} \approx 3P_{e,1}^2 \tag{173}$$

$$P_{e,3} \approx 10P_{e,1}^3 \tag{174}$$

$$P_{e,4} \approx 35P_{e,1}^4. \tag{175}$$

The optimum number of diversity paths will depend on a variety of considerations, among them the available bandwidth and transmitter power, system complexity, and the source of errors. When the errors are caused by noise it is possible to realize a certain minimum total average signal power for a specified error probability $P_{e,m}$, by appropriate choice of m. As shown by Pierce[18] and Harris,[19] the minimum total average signal power is attained for any specified error probability when m is so chosen that in each diversity channel $\bar{\rho} \approx 3$, or about 5 db, for binary FM with dual filter noncoherent detection. The number of diversity paths required to realize the minimum total average signal power is rather large, and the signal power reduction that can be realized with more than four paths is fairly small. For example, Pierce[18] shows that for an error probability $P_{e,m} = 10^{-4}$, the minimum average signal power is realized with $m = 16$, for which the total signal-to-noise ratio is 16.7 db, corresponding to a signal-to-noise ratio per channel of 4.7 db ($\bar{\rho} = 2.95$). With $m = 1$ the average signal-to-noise ratio is 40 db and with $m = 4$ is 19.4 db. Hence only a small additional reduction in signal power is realized when the number of diversity paths is increased from $m = 4$ to $m = 16$.

7.9 *Error Probabilities with Selection Diversity*

Equal gain diversity as considered above entails a linear addition of the baseband outputs of the various demodulators, and would be less effective in conjunction with nonlinear demodulation methods, such as binary FM with frequency discriminator detection. With the latter method, switch or selection diversity reception would probably be preferable, in which only the receiver having the largest signal is selected. With this method the following relations apply for m-diversity transmission when the errors are caused by noise and when receiver selection is based on the largest carrier signal at the detector input[8]

$$P_{e,m} \approx 2^{m-1} m! P_{e,1}{}^{m} \tag{176}$$

$$P_{e,2} \approx 4 P_{e,1}{}^{2} \tag{177}$$

$$P_{e,3} \approx 24 P_{e,1}{}^{3} \tag{178}$$

$$P_{e,4} \approx 192 P_{e,1}{}^{4}. \tag{179}$$

For equal error probability, the average signal power with selection diversity must be greater than with optimum diversity by a factor equal to the mth root of the ratio of the factors in (176) and (172). The power must thus be increased by 0.62, 1.27 and 1.85 db for $m = 2$, 3 and 4, respectively.

7.10 *Multiband Digital Transmission*

The curves in Figs. 21 and 22 suggest that for a given total transmitter power and channel bandwidth, the error probability can be reduced by transmitting at a slower rate over each of a number of narrower channels in parallel. An approximate optimum bandwidth for each channel would be such that $P_e^{(1)} + P_e^{(2)}$ is minimized. This can be accomplished with separate transmitters and receivers for each channel, such that mutual interference between channels is avoided. Hence the adverse effects of selective fading can be overcome with the aid of more complicated terminal equipment, without the need for increased signal power or channel bandwidth.

An alternative method that is simpler in implementation is to transmit the combined digital wave from the parallel channels by frequency or phase modulation of a common carrier, as ordinarily used for transmission of voice channels in frequency division multiplex. This method entails some mutual interference between channels, as well as greater channel bandwidth and carrier power than with direct digital carrier modulation, as discussed below.

With the above method, the spectrum of the modulated carrier wave will have greater bandwidth than with direct digital carrier modulation. To avoid excessive transmission distortion of the combined wave, the bandwidth between transmitter and receiver must be at least twice that with digital carrier modulation. Hence, at least 3 db greater average carrier power is required in order that the noise threshold level of the common channel be comparable with that of direct digital carrier modulation.

With such multiband transmission, intersymbol interference owing to selective fading is avoided, in exchange for mutual interference between the various channels owing to intermodulation distortion caused by selective fading. Such intermodulation distortion is dealt with elsewhere (this issue, part 2) for a modulating wave with the properties of random noise, which is approximated with a large number of binary channels in frequency division multiplex. The results indicate that under this condition intermodulation distortion will cause less transmission impairment than does intersymbol interference in direct digital transmission. Hence multiband transmission by common carrier modulation permits a reduction in error probability in exchange for at least a twofold increase in bandwidth and carrier power. However, this reduction in error probability may be less than can be realized with direct digital carrier modulation in conjunction with a twofold increase in bandwidth and signal power with dual diversity.

Error probabilities in binary multiband transmission by frequency modulation of a common carrier are dealt with by Barrow[21] on the premise of slow flat fading over the combined band, so that only errors owing to noise need be considered and intermodulation distortion can be disregarded.

VIII. SUMMARY

The objective of this analysis has been to develop a transmission and modulation theory for troposcatter systems, applicable to digital transmission by AM, FM and PM at any speed and based on a realistic idealization of troposcatter transmittance properties. The basic model, together with the analytical procedure and certain basic assumptions, are reviewed here.

8.1 *Troposcatter Transmittance*

Based on certain physical considerations, an idealized multipath transmittance model is developed in which the received component waves vary at random in amplitude and phase and have transmission delays owing to path length differences which vary linearly with angular deviation from the mean path with maximum deviations $\pm\Delta$ from the mean delay. With this type of model, a Rayleigh probability distribution is obtained for the envelope of a received carrier wave in conformance with observations.

To facilitate determination of transmission performance, two basic statistical parameters are required aside from the signal-to-noise ratio at the receiver. One of these is the autocorrelation function of envelope variations with time at a given frequency. The other is the autocorrelation function with respect to frequency at a fixed time.

The first of these, the time autocorrelation function, depends on the rapidity of changes in the atmospheric structure within the common antenna volume. It has been determined by a number of observations with some theoretical support, as given in certain publications.

The second basic parameter, the autocorrelation function with respect to frequency, has been determined by observation on a particular link. These observations conform well with the autocorrelation function determined analytically herein on the premise that the maximum delay deviation $\pm\Delta$ noted above is given by the path length differences based on the beam angles between the 3-db loss points.*

With the aid of this idealized model, endowed with the above basic parameters, as determined by observation or theory, it is possible in

* This conclusion appears to be supported by the results of recent measurements on a 100-mile path.[24]

principle to determine analytically the associated idealized transmission performance with any modulation method. Though an exact solution is possible in principle, it appears intractable and is not essential for engineering purposes. An approximate solution for transmission at any digital rate is derived herein. To this end certain basic statistical parameters are determined from the above two autocorrelation functions.

8.2 *Variations in Transmittance with Time*

In Section II, distributions are given for the time rate of change in the envelope and for the first and second derivatives of the phase function. These probability distributions permit approximate evaluation of changes in the envelope, phase and frequency over a signal or pulse interval for narrow-band signal spectra.

8.3 *Variations in Transmittance with Frequency*

The corresponding probability distributions with respect to variations in transmittance with frequency are given in Section III and permit approximate determination of random attenuation and phase distortion over the band of the signal spectra owing to the selectivity of fading. From these random variations it is possible to determine the corresponding pulse distortion together with resultant intersymbol interference in carrier pulse trains and error probability in the absence of noise.

8.4 *Errors from Selective Fading*

As a next step in the determination of error probability, an approximate evaluation is made in Section IV of the probability of errors from intersymbol interference with selective Rayleigh fading in the absence of noise. In a first approximation it turns out that attenuation distortion can be neglected in comparison with phase distortion. Furthermore, the latter can be approximated by a component of quadratic phase distortion, or corresponding linear delay distortion. Intersymbol interference owing to quadratic phase distortion is determined for various carrier modulation methods, and an approximate relation is derived for the resultant error probability in the absence of noise.

8.5 *Errors from Nonselective Rayleigh Fading*

With transmission at sufficiently slow rates, errors can occur in the absence of noise, owing to changes in amplitude, phase or frequency over

a pulse interval, caused by nonselective Rayleigh fading. The probability of errors on this account is determined in Section V on the approximate basis that changes over a pulse interval are proportional to the time derivatives of the amplitude, phase or frequency, depending on the modulation method. Comparison with available exact solutions for phase modulation shows that the inaccuracy resulting from this approximation is inappreciable.

8.6 *Errors from Random Noise*

In Section VI expressions are given for the probability of errors from random noise with flat Rayleigh fading, as derived in various publications for different digital carrier modulation methods. In addition, an expression is derived for error probability with rapid Rayleigh fading in conjunction with slow log-normal fading, as encountered on troposcatter links.

8.7 *Combined Error Probability*

In the final Section VII the combined error probability is determined on the approximate basis that it is the sum of the error probabilities for the three basic sources assumed above. Charts are presented from which can be determined the approximate combined error probabilities for binary phase and frequency modulation over a single path, and approximate expressions are given for the error probability with diversity transmission over independently fading paths.

8.8 *Basic Approximations*

The idealized model of troposcatter transmission assumed herein is of course an approximation, as are the idealizations regarding the performance of the carrier modulation methods. Even with exact mathematical analysis based on this model, the predicted performance would not conform entirely with that observed on actual systems.

In determining error probability from the idealized model, two basic approximations were used to obtain numerical results. One is that the maximum departures $\pm\Delta$ from the mean transmission delay can be determined from the beam angles taken between 3-db loss points. On short links with narrow-beam antennas, these are virtually equal to the free-space antenna beam angles, but for long links are greater owing to beam broadening by scatter. The second approximation is that errors from distortion owing to selective fading are caused principally by a

quadratic component of phase distortion. This is the first component that gives rise to distortion in a power series expansion of a nonlinear phase characteristic as a function of the frequency from the carrier.

The same two basic approximations have been used in a companion paper (this issue, part 2) in a determination of intermodulation noise in analog transmission by FM of signals with the properties of random noise. Theoretical predictions based on free-space beam angles are in this case in reasonable agreement with measurements on two tropo-scatter links 185 and 194 miles in length, with narrow-beam antennas. Measurements on links 340 and 440 miles long give intermodulation noise that would correspond to beam angles and maximum delay differences $\pm\Delta$ that are greater than for free space by factors of about 1.35 and 2.15, respectively.

The above measurements also show that as the bandwidth increases, actual intermodulation noise will be progressively smaller than predicted on the premise of quadratic phase distortion. Translated to digital transmission, the error probabilities $P_e^{(1)}$ owing to selective fading as determined here on the premise of quadratic phase distortion would represent an upper bound, that should conform well with actual error probabilities when the latter do not exceed about 10^{-2} in Figs. 21 and 22.

8.9 *Comparison with Recent Related Publications*

Since the completion of the galley proof of this paper an article by Bello and Nelin[22] has appeared, dealing with errors in binary transmission owing to frequency selective fading by a different analytical procedure than used here. Numerical results are presented for error probabilities in dual and quadruple diversity transmission by binary FM with dual filter incoherent detection and binary PM with differential phase coherent detection. These results are based on an assumed Gaussian correlation function, or power spectrum, of the selectivity of fading with frequency. A comparison is made below of the above numerical results with those obtained on similar premises from relations presented here.

For a Gaussian power spectrum of correlation bandwidth B_c as used in the above paper, the corresponding value of σ^2 in (18) is $\sigma^2 = 2(\pi B_c)^{-2}$. Expression (55) applies with $b_2/b_0 = \sigma^2$ in place of $\Delta^2/3$. With this substitution and with $T = \hat{B}^{-1}$, expression (101) and Fig. 17 apply, with $\Delta \cdot \hat{B} = 0.79(B_cT)^{-1}$, where $(B_cT)^{-1}$ is the parameter appearing in Figs. 5 and 9 of the above paper for the irreducible error probabilities.

Binary FM with dual filter detection as assumed in the above paper can be considered equivalent to ideal complementary binary AM over

each of two channels. When the frequency selectivity of fading is sufficient to cause errors in one or the other of these channels, the above method is essentially equivalent to dual diversity transmission by AM over two independently fading channels. On this basis, binary FM with dual diversity and dual filter noncoherent detection is approximately equivalent to binary AM with quadruple diversity. The error probabilities determined on the latter premise with $\Delta \cdot \hat{B} = 0.79(B_c T)^{-1}$ in (101), or in Fig. 17, in conjunction with (172) for $m = 4$, conform reasonably well with those given in Fig. 5 for dual diversity with $\psi = 0$ and $n = 1$. Complete agreement is not possible for the reason that the results in Fig. 5 assume a rectangular shape of undistorted pulses, whereas the present analysis is based on a more realistic pulse shape with a raised cosine spectrum, as indicated in Fig. 13.

In the case of binary PM with differential phase detection, the relations presented here with $\Delta \cdot \hat{B} = 0.79(B_c T)^{-1}$ yield error probabilities that are significantly smaller than those given in Fig. 9 of the above paper. This is to be expected, since the present relations are based on detection with an optimum threshold level, whereas those in the above paper assume zero threshold, which is not the optimum owing to the presence of a substantial bias component in the demodulator output, when pulse distortion is pronounced.[13] Moreover, the shapes of the undistorted pulses are different, as noted above.

It is evident from the above considerations that apparently unrelated and possibly misleading results can be obtained unless comparisons are made of binary modulation methods of equal bandwidths with optimum implementation of each, as was done in Fig. 17.

The above article called attention to another paper[23] by the same writers that refines Voelcker's original analysis[9] of errors in transmission over narrow-band channels owing to transmittance variations with time. Their results show that for a Gaussian power spectrum of the fading rate as assumed herein, Voelcker's analysis is exact, though this is not true for all forms of power spectra.

IX. ACKNOWLEDGMENTS

Results have been quoted herein from a number of papers dealing with troposcatter transmission properties and with error probabilities owing to random noise in conjunction with Rayleigh fading. The principal new results pertain to error probabilities at sufficiently high digital rates for selective fading to be important. In determining these error probabilities, advantage was taken of results published by S. O. Rice on the probability densities of the first and second time derivatives of

the phase of random narrow-band noise. The writer is also indebted to him for helpful suggestions resulting in certain mathematical simplifications. He also had the advantage of a discussion with I. Jacobs and D. S. Bugnolo, who pointed out certain basic limitations of the present idealized statistical model of troposcatter transmission, and he is also indebted to several other associates for helpful critical comments.

APPENDIX

Transmittance of Troposcatter Channels

Owing to the differences in path length from transmitter to receiver via the various heterogeneities in the common volume, the various components of the received wave arrive with different delays. For analytical purposes it is convenient to assume a certain mean reference path with delay T_0 and to express the transmission delay via other paths relative to the delay T_0. Actually there will be a large number of paths with the same delay T_0 as the mean path and a large number of paths for each other delay. In the present analysis the approximate model indicated below is assumed, with a single vertical scatter plane midway between transmitter and receiver.

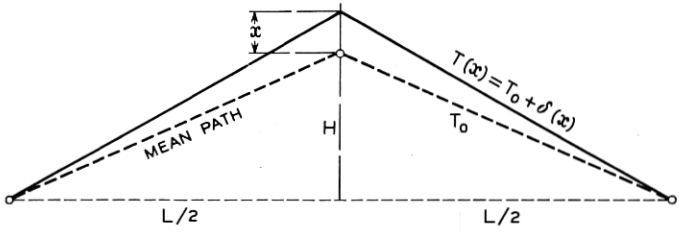

The amplitude of the wave component arriving over a path at the distance x above the mean path is taken as $A(x,t)$ and the delay over this path as

$$T(x) = T_0 + \delta(x).$$

The wave component arriving via this path is then

$$e_x(\omega,t) = A(x,t) \cos \omega[t - T_0 - \delta(x)]. \tag{180}$$

Let L be the distance between transmitter and receiver and H the height of the mean path. In this case

$$\delta(x) = s(x)/v \tag{181}$$

where v is the velocity of propagation and $s(x)$ the path length difference given by

$$s(x) = \left[\frac{L^2}{4} + (H + x)^2\right]^{\frac{1}{2}} - \left(\frac{L^2}{4} + H^2\right)^{\frac{1}{2}}. \tag{182}$$

In actual systems $H \ll L$. Furthermore, the maximum value $\hat{x}$ of x is ordinarily much smaller than H. On these premises the following approximation applies

$$\delta(x) = (2H/Lv)x = x/c \tag{183}$$

where $c = vL/2H$.

It will further be assumed that there is an infinite number of paths, in which case the received wave becomes

$$e(\omega,t) = \int_{-\hat{x}}^{\hat{x}} A(x,t) \cos \omega(t - T_0 - x/c)\, dx \tag{184}$$

$$\begin{aligned} &= \cos \omega(t - T_0) \int_0^{\hat{x}} [A(x,t) + A(-x,t)] \cos (\omega x/c)\, dx \\ &\quad + \sin \omega(t - T_0) \int_0^{\hat{x}} [A(x,t) - A(-x,t)] \sin (\omega x/c)\, dx. \end{aligned} \tag{185}$$

It will now be assumed that

$$\int_0^{\hat{x}} [A(x,t) + A(-x,t)]\, dx = 0. \tag{186}$$

This appears to be an appropriate physical requirement, for the reason that reflections occur as a result of variations in the electrical properties of an elementary volume, relative to that of the common volume. No reflections occur with a uniform common volume. In a heterogeneous common volume, each positive reflection must be accompanied by an equal negative reflection, which is reflected in condition (186). Moreover, under this condition there is no reflection along the mean path of the transmitted beam. That is, with $x = 0$ in (185), $e(t) = 0$ provided (186) applies.

Condition (186) can be insured if the following Fourier series representations are used for $x \leqq \hat{x}$

$$A(x,t) + A(-x,t) = \sum_{m=1}^{\infty} a(m,t) \cos m\pi x/\hat{x} \tag{187}$$

and

$$A(x,t) - A(-x,t) = \sum_{m=1}^{\infty} b(m,t) \sin m\pi x/\hat{x}. \tag{188}$$

With $m = 1, 2, 3$, etc., as above, the area under each harmonic component vanishes, such that condition (186) is satisfied.

With (187) and (188) in (185), the following relation is obtained

$$e(\omega,t) = \cos \omega(t - T)U(\omega,t) + \sin \omega(t - T)V(\omega,t) \tag{189}$$

where

$$U(\omega,t) = \sum_{m=1}^{\infty} a(m,t) \int_0^{\hat{x}} \cos m\pi x/\hat{x} \cos \omega x/c \, dx \tag{190}$$

$$V(\omega,t) = \sum_{m=1}^{\infty} b(m,t) \int_0^{\hat{x}} \sin m\pi x/\hat{x} \sin \omega x/c \, dx \tag{191}$$

Evaluation of the integrals yields the following expressions

$$U(\omega,t) = \sum_{m=1}^{\infty} \tfrac{1}{2} A(m,t) \left[\frac{\sin (m\pi - \omega\Delta)}{m\pi - \omega\Delta} + \frac{\sin (m\pi + \omega\Delta)}{m\pi + \omega\Delta} \right] \tag{192}$$

$$V(\omega,t) = \sum_{m=1}^{\infty} \tfrac{1}{2} B(m,t) \left[\frac{\sin (m\pi - \omega\Delta)}{m\pi - \omega\Delta} - \frac{\sin (m\pi + \omega\Delta)}{m\pi + \omega\Delta} \right] \tag{193}$$

where

$$\begin{aligned} A(m,t) &= \hat{x}a(m,t) \\ B(m,t) &= \hat{x}b(m,t) \\ \Delta &= \hat{x}/c. \end{aligned} \tag{194}$$

It will be noted that Δ is the maximum departure from the mean delay T_0.

In evaluation of (192) and (193) it is convenient to introduce a new reference frequency ω_0 in place of 0, and to choose this reference frequency such that

$$\omega_0\Delta = n\pi. \tag{195}$$

Thus

$$\omega\Delta = n\pi + u\Delta \tag{196}$$

where $-\pi < u\Delta < \pi$, and u is the deviation in frequency from ω_0.

The functions (192) and (193) are then replaced by

$$\begin{aligned} U(u,t) = \sum_{m=1}^{\infty} \tfrac{1}{2} A(m,t) \Bigg\{ &\frac{\sin [(m - n)\pi - u\Delta]}{(m - n)\pi - u\Delta} \\ &+ \frac{\sin [(m + n)\pi + u\Delta]}{\sin (m + n)\pi + u\Delta} \Bigg\} \end{aligned} \tag{197}$$

$$V(u,t) = \sum_{m=1}^{\infty} \tfrac{1}{2}B(m,t) \left\{ \frac{\sin [(m-n)\pi - u\Delta]}{(m-n)\pi - u\Delta} - \frac{\sin [(m+n)\pi + u\Delta]}{\sin (m+n)\pi + u\Delta} \right\}. \tag{198}$$

In troposcatter transmission it turns out that m is of the order of 100 to 1000. For this reason the second terms in the above series, in $(m + n)\pi$, can be neglected. With this simplification and with $m - n = j$, expressions (5) and (6) are obtained.

Expression (189) can then be written in the form

$$e(\omega,t) = r(u,t) \cos [\omega(t - T) - \varphi(u,t)] \tag{199}$$

where r and φ are given by (3) and (4).

The channel transmittance is accordingly given by (2).

REFERENCES

1. Bullington, K., Radio Propagation Fundamentals, B.S.T.J., **36,** May, 1957, p. 593.
2. Crawford, A. B., Hogg, D. C., and Kummer, W. H., Studies in Tropospheric Propagation Beyond the Horizon, B.S.T.J., **38,** September, 1959, p. 1067.
3. Ortwein, N. R., Hopkins, R. U. F., and Pohl, J. E., Properties of Tropospheric Scatter Fields, Proc. IRE, **49,** April, 1961, p. 788.
4. Rice, S. O., Distribution of the Duration of Fades in Radio Transmission, B.S.T.J., **37,** May, 1958, p. 581.
5. Clutts, C. E., Kennedy, R. N., and Trecker, J. M., Results of Bandwidth Tests on the 185-Mile Florida-Cuba Scatter Radio System, IRE Trans. on Comm. Systems, **9,** December, 1961, p. 434.
6. Beach, C. D., and Trecker, J. M., A Method of Predicting Interchannel Modulation Due to Multipath Propagation in FM and PM Tropospheric Radio Systems, B.S.T.J., **42,** January, 1963, p. 1.
7. Turin, G. L., Error Probabilities for Binary Symmetric Ideal Reception Through Nonselective Slow Fading and Noise, Proc. IRE, **46,** September, 1958, p. 1603.
8. Pierce, J. N., Theoretical Diversity Improvement in Frequency Shift Keying, Proc. IRE, **46,** May, 1958, p. 903.
9. Voelcker, H. B., Phase-Shift Keying in Fading Channels, JIEE, **107,** January, 1960, p. 31.
10. Zadeh, L. A., Frequency Analysis of Variable Networks, Proc. IRE, **38,** March, 1950, p. 291.
11. Price, R., A Note on the Envelope and Phase-Modulated Components of Narrowband Gaussian Noise, IRE Trans. on Information Theory, **1,** September, 1955, p. 9.
12. Rice, S. O., Properties of Sine Wave Plus Random Noise, B.S.T.J., **27,** January, 1948, p. 109.
13. Sunde, E. D., Pulse Transmission by AM, FM and PM in Presence of Phase Distortion, B.S.T.J., **40,** March, 1961, p. 353.
14. Sunde, E. D., Ideal Binary Pulse Transmission by AM and FM, B.S.T.J., **38,** November, 1959, p. 1357.
15. Lawton, J. G., Comparison of Binary Data Transmission Systems, Proc. of the Second National Conference on Military Electronics, 1958.
16. Reiger, S., Error Probabilities in Binary Data Transmission Systems in Presence of Random Noise, Convention Record of IRE, Part 8, 1953, p. 72.

17. Bennett, W. R., and Salz, J., Binary Data Transmission by FM over a Real Channel, B.S.T.J., **42,** September, 1963, p. 2387.
18. Brennan, D. G., Linear Diversity Combining Techniques, Proc. IRE, **47,** June, 1959, p. 1075.
19. Pierce, J. N., Theoretical Limitations on Frequency and Time Diversity for Fading Binary Transmissions, IRE Trans. on Comm. Systems, **9,** June, 1961, p. 186.
20. Harris, D. P., Techniques for Incoherent Scatter Communications, IRE Trans. on Comm. Systems, **10,** June, 1962, p. 154.
21. Barrow, B. B., Error Probabilities for Telegraph Signals Transmitted on a Fading FM Carrier, Proc. IRE, **48,** September, 1960, p. 1613.
22. Bello, P. A., and Nelin, D. B., The Effect of Frequency-Selective Fading on the Binary Error Probabilities of Incoherent and Differentially Coherent Matched Filter Receivers, IEEE Trans. on Comm. Syst. **11,** June, 1963 (issued in October), p. 170.
23. Bello, P. A., and Nelin, D. B., The Influence of Fading Spectrum on the Binary Error Probabilities of Incoherent and Differentially Coherent Matched Filter Receivers, IRE Trans. on Comm. Syst., **10,** June 1962, p. 160.
24. Patrick, W. S., and Wiggins, M. J., Experimental Studies of the Correlation Bandwidth of the Tropospheric Scatter Medium at Five Gigacycles, IEEE Trans. Aerosp. and Nav. Elect., June, 1963.